DESIGN AND FABRICATION OF LOW-SPEED WATER TUNNEL FOR FLOW VISUALIZATION

By:

Ihtisham Muhammad Arif Khan
Hassnain Ali
Muhammad Hammad Asghar
Nauman Naeem

Project Supervisor

(Mr. Bilal Haider)

Project Co-Supervisor

(Mr. Ammar Akram)

MECHANICAL ENGINEERING DEPARTMENT
HITEC UNIVERSITY, TAXILA

July 2022

DESIGN AND FABRICATION OF LOW-SPEED WATER TUNNEL FOR FLOW VISUALIZATION

FINAL YEAR PROJECT REPORT

SESSION 2018

THESIS IS SUBMITTED TO THE FACULTY OF THE DEPARTMENT OF MECHANICAL ENGINEERING, HITEC UNIVERSITY, TAXILA IN PARTIAL FULFILLMENT OF THE REQUIREMENTS FOR THE DEGREE OF BACHELOR OF SCIENCE IN MECHANICAL ENGINEERING

DEPARTMENT OF MECHANICAL ENGINEERING

ACKNOWLEDGEMENTS

Thanks to Almighty Allah for showering His blessings upon us and giving us strength to work on this project. We want to thank our project supervisor **Sir Bilal Haider** for their technical and innovative thinking that guided us at every step to complete this project. We also want to thank our Co-Supervisor **Sir Muhammad Ammar Akram** for being available at every hour to guide us. Thanks to our committee members **Dr. Fahad Butt** and **Miss Munazza Haq** for making sure that we give our best to this project. Finally, we want to thank our parents for always encouraging and supporting us in our tough times. Thanks to everyone who helped us and prayed for us.

Abstract:

The Hydrodynamic Water Tunnel serves as an equipment that helps to study the behavior of hydrodynamic forces, boundary layer, vortex shedding, lift-drag forces generated due to submerged objects. This paper presents the design and fabrication of the water tunnel's key components and the methodologies involved in fabrication, for example, design of baffles, Pump, Test Section, and the Diffuser/Nozzle. The Water Tunnel has an observation chamber of Width Height and Length of 270 mm, 260 mm, 9144 mm respectively with flow velocity of 0.7 m/s. The pump selected for the Water Tunnel is a centrifugal water pump (10 hp) with a pumping capacity of 2200 LPM at a maximum head of 120 ft. This Water Tunnel will be used for the testing of various specimens to determine their flow patterns, stability, and hydrodynamics. Experimentation has been performed using on this Water Tunnel with a test rig of heat exchanger tube bundles with cross-arrangement to study the behavior of Fluid Elastic Instability generated because of fluid structure interaction.

List of figures:

List of tables:

Table of Contents:

Chapter 1 Introduction:

A water tunnel is a hydrodynamic experimental facility used to investigate the flow behavior and hydrodynamic forces acting on submerged bodies. Its operating principle is similar to that of a wind tunnel, except that water is used as the working fluid. This makes the flow visualization process easy and accessible for low Reynolds no. flow. i.e., Using (Dye injection or tracers when using Particle Image Velocimetry PIV)[1].

The water tunnel is much simpler in all ways because of its simple construction and design in comparison with a wind tunnel. A wind tunnel uses a series of specially designed blades to enhance the flow and a compressor that pumps the air. But, as for water tunnel the water is pumped and recirculated inside the flume by only a centrifugal pump that passes through a series of pipes and components with changing cross-sectional.

Water tunnels are widely used because they provide a versatile experimental platform for flow visualization and the investigation of hydrodynamic phenomena over a broad range of flow conditions. Although computational fluid dynamics (CFD) provides valuable numerical predictions, experimental testing remains essential for validating numerical models under realistic flow conditions.[2] Simulations are being done on equipment to eliminate any form of error and validate it in real world conditions.

Chapter 2 Literature Review:

The Water Tunnel is a versatile piece of equipment that has been used by researchers to test the hydrodynamic effects of fluids on submerged bodies like Lift, Drag, Vortex-Induced Vibrations (VIV), Cavitation, and Skin Friction. Their popularity has been increasing due to more advances in Fluid Mechanics because flow visualization is easy to observe due to the high viscosity of water unlike the wind tunnel that operate at high speeds and dry observations are hard to comprehend.

There have been multiple variants of the water tunnel starting from the St. Anthony Falls High-Speed Water Tunnel [3] having a flow speed of 20 m/s, The Large Cavitation [4], [5] Channel for the testing of American Naval Torpedoes with a cross-section testing chamber area of 120 sq-inches, also other like the HYKAT [6], LOCAT [6] with bigger cross-sections. The large-scale water tunnels generate noise at sudden bends and cause sudden vibrations so to solve the Flow Noise Simulator [12] was Designed. Other Variants include the Circular test chamber of the Garfield Thomas Water Tunnel which is mostly used for a uniform velocity profile of the incoming flow against the test specimen [14].

These variants are further classified by the type of baffles used like the Cylindrical Baffle with a net, baffle-drop shaft structure, Novel Slot-baffle, and the Ventilated Corner Baffles.

Saeed et al. designed the water tunnel in an inlet plenum and reached the velocity of 0.5 m/s. Another low-speed water tunnel designed by Kalgutkar et al. has a working velocity of 0.21 m/s.

Name	**Ownership**	**Test Section Dimensions (in.)**	**Max. Speed (m/s)**	**Associated Literature**
Large Cavitation Channel (LCC)	NAVSEA, Carderock (USA)	120 x120	18	[4], [5]
HYKAT	HSVA (Germany)	110 x 63	12	[6]
LOCAT	MOERI (Korea)	110 x 70	15	[6]
St. Anthony Falls High-Speed Water Tunnel	University of Minnesota (USA)	7.4 x 7.4	20	[7]
Mini-LCC	University of Michigan (USA)	8.6 x 8.6	25	[8]
High-Speed Cavitation Tunnel (HiCaT)	University of New Hampshire (USA)	6 x 6	17	[9]
Tunnel de Cavitation	Ecole Navale (France)	7.6 x 7.6	15	[10]
Grand Tunnel Hydrodynamique (GTH)	Bassin d'Essais des Carènes (France)	44.9 x 44.9	20	[11]
Flow Noise Simulator (FNS)	Naval Systems Research Center (Japan)	91.7 x 91.7	15	[12]
9-inch Water Tunnel	University of Michigan (USA)	9 (diameter)	18	[13]
Garfield Thomas Water Tunnel	Pennsylvania State University (USA)	48 (diameter)	18	[14]
12-inch Water Tunnel	Pennsylvania State University (USA)	12 (diameter)	24	[15] [16] [17]

6-inch Water Tunnel	Oklahoma State University (USA)	6 x 6	12	[18]
	Japan Society of Mechanical Engineers (JSME)	400mm x 167 mm	1.5	[19]
Aerolab Educational Wind Tunnel	California State University, Maritime Academy (CSUMA)	6”x12”x12”	0.32-0.65 ft/s	[20]
low turbulence recirculating water tunnel	Oklahoma State University	152mm x 152mm	10 m/s	[18]

TABLE 2-1LIST OF EXISTING WATER TUNNELS

Types of Water Tunnels made	Associated Literature
Low Speed	Design and development of low-speed water tunnel[21]
Recirculating	Design and Validation of a Recirculating, High-Reynolds Number Water Tunnel[22]
Open Water Flume	Open water flume for fluid mechanics lab[23], [24]
High-Speed	Chalmers Open Digital Repository: Design of Contraction, Test Section, and Diffuser for a High-Speed Water Tunnel[25]

TABLE 2-2 LIST OF TYPES OF WATER TUNNELS MADE

Rod Bundle	Diameter of rod mm	P/D	Test Chamber mm	Rod Material	Length of Rod mm	Literature Reviewed
5 x 5	10.25	1.26	101.6 x 101.6 x1826	fluorinated ethylene-propylene (FEP)	1270	(Xing Li et al 2018)

3 x 3	9.5	1.32	65 x 65 x 1200	(FEP)	1100	(Elvis E et al 2008)
9x 17	**12.7**	**1.54**	**300 x 300**	**(FEP)**	**295**	**(Akram, Muhammad Ammar, et al. 2021)**

TABLE 2-3 LIST OF LITERATURE FOR TUBE BUNDLES

Type of Baffles Used	Associated Literature
Cylindrical Baffle with a net	Design and Analysis of Low-Speed Water Tunnel for Flow Visualization of Bluff Body [26]
baffle-drop shaft structure	Experimental investigation of hydraulic characteristics and energy dissipation in a baffle-drop shaft [27]
Novel Slot-Baffle	Liquid Sloshing Damping in an Accelerated Tank Using a Novel Slot-Baffle Design [28]
Ventilated Corner Baffles	Ventilated Corner Baffles to Assist Upstream Passage of Small-Bodied Fish in Box Culverts [29]

TABLE 2-4 BAFFLES USED IN WATER TUNNEL

Working Fluid	Dye	Associated Literature
Water	Milk and Food Coloring	Study by hydrodynamic visualizations of various processes for controlling separated flows [30]
Salt Water	Milk	Gravity currents produced by instantaneous releases of a heavy fluid in a rectangular channel [31]
Water	Dye	Some flow visualization experiments on the starting vortex[32]
Water	Ink	Disrupted states of vortex flow and vortex breakdown[33]

TABLE 2-5 TYPES OF DYE COMBINATION USED

Types of Testing	Purpose	Associated Literature
Dynamic Testing	unsteady aerodynamic	Development and Use of a Dynamic-Testing

	effects associated with aircraft motion	Capability for the DSTO Water Tunnel[34]
Aerodynamic Testing	for providing validation data for computational-fluid-dynamics analyses of a flow	An Assessment of the Usefulness of Water Tunnels for Aerodynamic Investigations[35]
Tangent ogive testing	Aerodynamic maneuvering slender bodies	Temporal evolution of the flow of fields over a pitching tangent ogive cylinder [36]

TABLE 2-6 TYPES OF TESTING DONE ON WATER TUNNEL

Method	Tracers	Associated Literature
Dye Injection	Colored Dye	An investigation into the use of GAMA water tunnel for visualization of vortex breakdown on the delta wing [37]
dye and hydrogen bubble techniques	Hydrogen Bubbles	Water Tunnel Flow Visualization of Vortex Breakdown Over the F/A-18[38]
laser-Doppler anemometry (LDA) and particle image velocimetry (PIV)	Glass spheres	Investigations on controlled transition development in a laminar separation bubble by means of LDA and PIV[39]
coupling a flame ionization detector (FID) and hot-wire anemometer (HWA),	Ethane	Wind-tunnel experiments on atmospheric heavy gas dispersion: Metrological aspects[40]

TABLE 2-7 VISUALIZATION METHODS USED FOR WATER TUNNEL

Chapter 3 Theoretical Background

3.1. Basic Definitions:

3.1.1. Mass Flow Rate:

The mass of water flowing upstream from area A and at velocity V.

$$Q = A \times V \ldots\ldots\ldots\ldots\ldots\ldots\ldots\ldots\ldots\ldots \text{(1)}$$

3.1.2. Reynolds Number:

The ratio between the inertial forces and the viscous forces.

$$Re = \frac{VD_h}{\nu} \ldots\ldots\ldots\ldots\ldots\ldots\ldots\ldots\ldots \ldots \text{(2)}$$

3.1.3. Froude number:

The ratio between the flow of inertial forces to the external field forces

$$Fr = \frac{(v)}{\sqrt{gd}} \ldots\ldots\ldots\ldots\ldots\ldots\ldots\ldots\ldots\ldots \text{(3)}$$

3.1.4. Haaland's Equation:

It is a relationship used as an alternative to determine head loss instead of using the moody chart.

$$\frac{1}{\sqrt{f}} = -1.8 \log\left[\left(\frac{\Sigma/_D}{3.7}\right)^{1.11} + \frac{6.9}{Re}\right] \ldots\ldots\ldots \text{(4)}$$

3.1.5. Major Losses:

Occur in Pipes, Conduits and Ducts.

$$h_L = f\frac{L}{D}\frac{V^2}{2g} \ldots\ldots\ldots\ldots\ldots\ldots\ldots\ldots\ldots \text{(5)}$$

3.1.6. Minor Losses:

Used to Head Losses in Bends, valves, sudden expansions, and contraptions.

$$h_L = K\frac{V^2}{2g} \ldots\ldots\ldots\ldots\ldots\ldots\ldots\ldots\ldots \text{(6)}$$

3.1.7. Power:

Tell us the Centrifugal Pump's Capacity.

$$Power = P = \rho \times g \times H \times Q \ldots\ldots\ldots \text{(7)}$$

Chapter 4 Design:

Before discussing the detailed design of the Water Tunnel. It is imperative to give summary of the components involved in the Water Tunnel. (1) Centrifugal Pump provides the plumbing subsystem with water, (2) Nozzle increases the flow velocity which enters the Flume (3) Baffle creates a uniformity in flow for easy visualization, (3) Diffuser creates a union between different cross-section parts of the water flume, (4) Test Section acts as a viewing chamber (5) Gate Valve is used to create the flowrate of flow coming into the Water Flume.

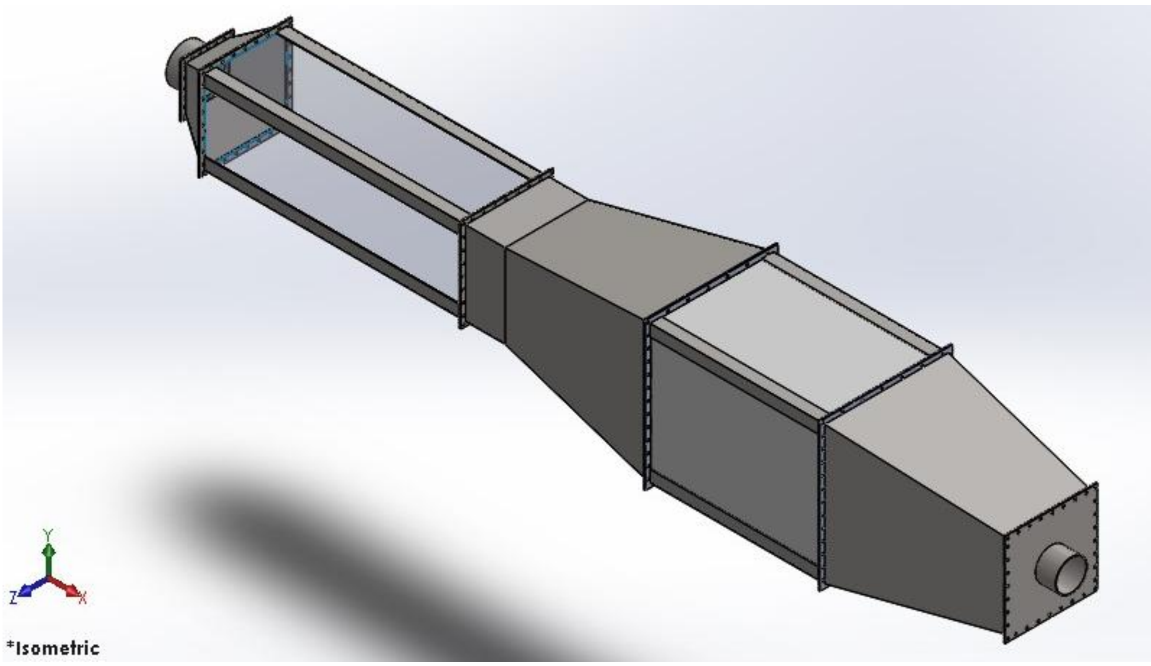

FIGURE 4-1 WATER TUNNEL DESIGN MODEL

The design of each component in the water flume was optimized based on head losses so that the required velocity would be achieved in the desired section of the flume. The designed water tunnel has a closed loop flow means that the water that flows out of the flume is pumped back to flume inlet due to this there are always chances of instability which degrades the quality of the flow.

FIGURE 4-2 ACTUAL MODEL OF WATER TUNNEL

Each component of the Flume is designed with reference to its previous component simultaneously and iteratively.

4.1. Diffuser/Nozzle:

The Diffuser acts as a linear gradual expansion zone, and its design is crucial to the quality of the flow. The flat walled diffuser was used in the flume because of its simple geometry and fabrication method. The design geometry of the thin-walled diffuser is dependent upon Divergence angle of Diffuser.

The angle is chosen by taking into consideration of the head loss, at $\vartheta > 15$, Head loss is large due to flow separation, for $\vartheta < 5$ the Diffuser is too long and has too much friction Thus, more head loss. But, for angles between $5 < \vartheta < 15$ is most efficient for designing the Diffuser. For our case, our Divergence angle is 8.5°. Which is acceptable for better head loss.

The galvanized sheets have a high resistance to corrosion, which will consequently increase the life span of the apparatus. The thickness of the sheet is 1.5mm.

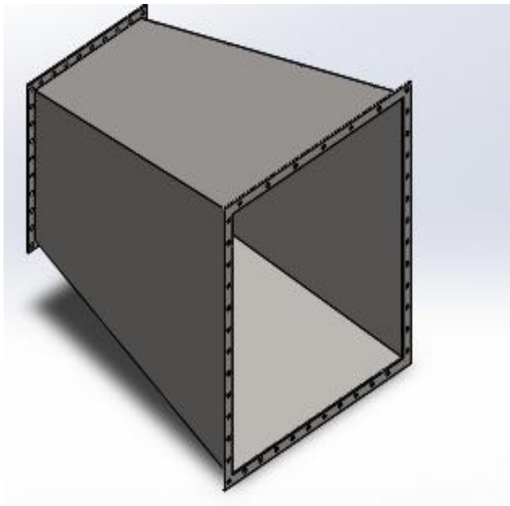

FIGURE 4-3 DIFFUSER DESIGN

FIGURE 4-3 ACTUAL MODEL OF DIFFUSER

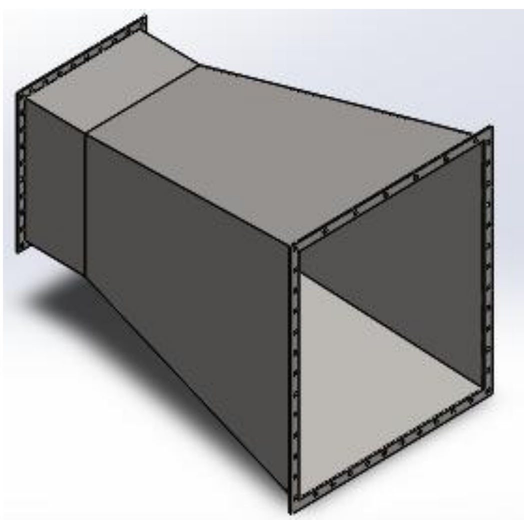

FIGURE 4-5 NOZZLE DESIGN

FIGURE 4-4 ACTUAL MODEL OF NOZZLE

4.2. Test Section:

The Test Section of the Water Tunnel has a cross-sectional area of 270 x 230 mm and a length of 0.9177 m. The dimension was decided to keep it in use for scale-down models of text specimens. The acrylic glass sheet is used for viewing chamber due to its Matching Reflective Index (MIR). The MIR of acrylic glass is greater than one approx. 1.48899. [41]

Other benefits of using acrylic sheets are.

- that thermal conductivity of the acrylic sheet is much higher than the glass.
- It is easy to remove dirt from the acrylic sheet as compared to ordinary glass.
- The density of acrylic sheets is 1.18 g/cm3[42] while the density of the normal glass is 2.58 g/cm3[43].

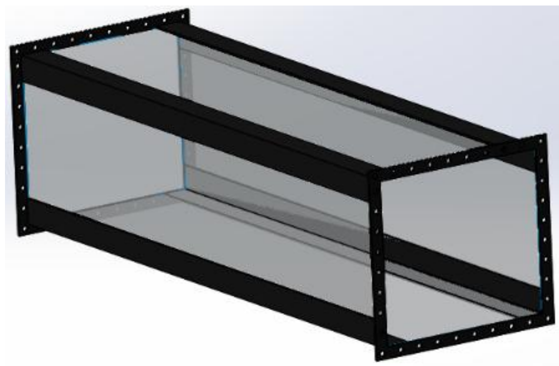

Figure 4-7 Test section design

FIGURE 4-5 ACTUAL MODEL OF TEST SECTION

4.3. Pipe:

The pipe used for the plumbing subsystem is PVC pipe of four'' diameter, ABS pipe was considered as well but due to lack of availability they were dropped.

4.4. Centrifugal Pump:

The Centrifugal Pump is used in the Tunnel. Because it is a Dynamic Pump, it means it has a continuous flow rate as compared to Positively Displaced Pumps (PDPs) [44]. Also, there are fewer vibrations generated. The power of the pump was determined by the following formula:

$Power = P = \rho \times g \times H \times Q$

Where:

H is the total Head Loss

ρ is the fluid's density

g is the gravitational const.

And Q is the flow rate at the Test Section

From the calculations 5.66 hp was determined with a Factor of Safety of 1.5 but due to the pump manufacturers do not have the required flowrate at 5 HP so instead we used a 10 HP based on its flowrate.

4.5. Baffles:

It is the most crucial part of Water Tunnel because it is responsible for converting the high-speed turbulent flow into laminar flow. The Baffles used for this Water Tunnel uses an array of multiple pipes that slow down its flow by means of friction between the fluid and pipes and due to contraction area that the space between the pipes that partially blocks the water. For the design process we considered the Head Loss and Reynolds No. to be the primary variables.

The problem encountered during the design was by increasing the no. of pipes in the baffles the Head loss increased dramatically so, this problem was solved by iterating the no. of pipes, pipe diameter and length of pipes several times until we found a desirable value of Head loss and the required Reynolds No.

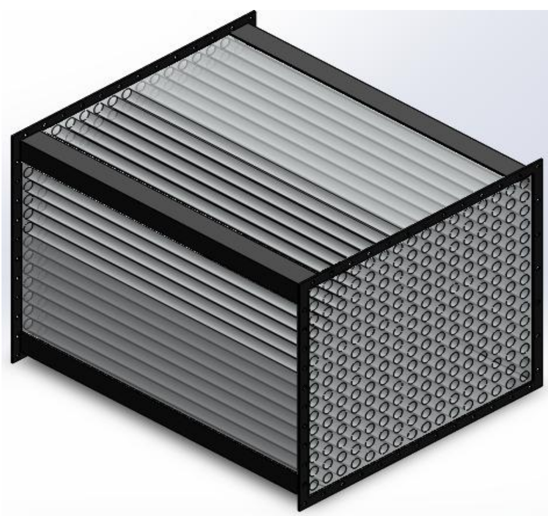

FIGURE 4-6 BAFFLES DESIGN

FIGURE 4-7 ACTUAL MODEL OF BAFFLES

Chapter 5 Calculations:

5.1. Test Section:

$$\text{Length of test section} = \text{L} = 36 \text{ inch} = 3\text{ft} = 0.9144 \text{ m}$$

$$\text{Width of test section} = \text{a} = 9 \text{ inch} = 0.229 \text{ m}$$

$$\text{Height of test section} = \text{b} = 9 \text{ inch} = 0.229 \text{ m}$$

$$\text{Velocity of test section} = \text{V} = 0.7 \text{ m/s}$$

$$\text{Kinematic Viscosity} = \nu = 0.8927 \times 10^{-6}$$

5.1.1. Flow Rate:

$$Q = A \times V$$

$$Q = (0.229 \times 0.229) \times 0.7$$

$$\mathbf{Q = 0.0367\ m^3/s}$$

5.1.2. Major Head Loss:

As,

$h_L = f\frac{L}{D}\frac{V^2}{2g}$……………………......(i)

$$Hydraulic\ dia = D_h = \frac{2ab}{a+b} = \frac{2(0.229)^2}{0.229 + 0.229} = 0.229\ m$$

And

$$Re = \frac{VD_h}{\nu} = \frac{0.7 \times 0.229}{0.8927 \times 10^{-6}} = 179568$$

So, the flow is Turbulent.

Now for head loss,

$$\frac{1}{\sqrt{f}} = -1.8 \log\left[\left(\frac{\Sigma/_D}{3.7}\right)^{1.11} + \frac{6.9}{Re}\right]$$

For Plastic drawn Tube.

$$\Sigma = 0.0015\ mm = 0.0015 \times 10^{-3}\ m$$

So,

$$\frac{1}{\sqrt{f}} = -1.8 \log\left[\left(\frac{0.0015 \times 10^{-3}/_{0.229}}{3.7}\right)^{1.11} + \frac{6.9}{179568}\right]$$

$$\frac{1}{\sqrt{f}} = 7.9393$$

$$f = 0.0159$$

Putting the values in eq (i).

$$h_L = 0.0159 \times \frac{0.914}{0.229} \times \frac{(0.7)^2}{2 \times 9.81}$$

$$\boldsymbol{Major\ Head\ Loss = h_L = 0.00158\ \mathrm{m}}$$

5.1.3. Volume:

Length of test section $= \mathrm{L} = 36$ inch $= 0.194$ m

Width of test section $= \mathrm{W} = 9$ inch $= 0.229$ m

Height of test section $= \mathrm{H} = 9$ inch $= 0.229$ m

Area $= \mathrm{L} \times \mathrm{W} = 9 \times 9 = 81\ inch^2$

Volume of test section $= \mathrm{V} = \mathrm{L} \times \mathrm{W} \times \mathrm{H} = 9 \times 9 \times 36$

$$\mathbf{V = 2916}\ \boldsymbol{inch^3}$$

$$\mathbf{Volume = V = 47.785\ liters}$$

5.2. Nozzle:

Width of Nozzle $= W_1 = 16.8$ inch $= 0.427$ m $\quad \therefore 1 = inlet$

Width of Nozzle $= W_2 = 9$ inch $= 0.229$ m $\quad 2 = outlet$

Height of Nozzle $= H_1 = 18.3$ inch $= 0.465$ m

Height of Nozzle $= H_2 = 9$ inch $= 0.229$ m

Length of Nozzle $= \mathrm{L} = 22.7$ inch $= 0.575$ m

As,

$Inlet\ flow\ rate = Q_1$

$Outlet\ flow\ rate = Q_2$

$Q_1 = Q_2 = Q = 0.0367\ m^3/s$ $\therefore for\ pipe\ in\ series$ $\therefore 2 = Test\ inlet$

$1 = Nozzle\ inlet$

$$A_1V_1 = A_2V_2$$

$$V_1 = \frac{A_2V_2}{A_1}$$

$A_1 = 0.427 \times 0.465 = 0.1986\ m^2$

So,

$$V_1 = \frac{(0.229)^2(0.7)}{0.1986}$$

$$\boldsymbol{V_1 = 0.18483\ \ m/s}$$

5.2.1. Minor Head Loss:

As,

$$Hydraulic\ dia = D_{h1} = \frac{2(W_1 \times H_1)}{\left((W_1 + H_1)\right)} = \frac{2(0.427)(0.465)}{0.427 + 0.465} = 0.4451\ m$$

And,

$$Hydraulic\ dia = D_{h2} = \frac{2(W_2 \times H_2)}{(W_2 + H_2)} = \frac{2(0.229)(0.229)}{0.229 + 0.229} = 0.229\ m$$

$$Re = \frac{VD_h}{\nu} = \frac{0.18483 \times 0.4451}{0.8927 \times 10^{-6}} = 92156$$

Now for head loss,

$$\frac{1}{\sqrt{f}} = -1.8 \log\left[\left(\frac{\Sigma/D_h}{3.7}\right)^{1.11} + \frac{6.9}{Re}\right]$$

For Galvanized iron.

$$\Sigma = 0.15\ mm = 0.15 \times 10^{-3}\ m$$

So,

$$\frac{1}{\sqrt{f_1}} = -1.8\log\left[\left(\frac{0.15\times 10^{-3}/_{0.4451}}{3.7}\right)^{1.11} + \frac{6.9}{92156}\right]$$

$$\frac{1}{\sqrt{f_1}} = 7.1427$$

$$f_1 = 0.0196$$

And,

$$\frac{1}{\sqrt{f_2}} = -1.8\log\left[\left(\frac{0.15\times 10^{-3}/_{0.229}}{3.7}\right)^{1.11} + \frac{6.9}{92156}\right]$$

$$\frac{1}{\sqrt{f_2}} = 6.9186$$

$$f_2 = 0.0208$$

$$f_{avg} = \frac{f_1 + f_2}{2} = \frac{0.0196 + 0.0208}{2} = 0.0202$$

As,

$$K = 2.61\sin\theta\left(1 - \frac{{D_{h2}}^2}{{D_{h1}}^2}\right)^2 + f_{avg}\frac{L}{d_{avg}}$$

$$d_{avg} = \frac{0.229 + 0.4451}{2} = 0.33705$$

So,

$$K = 2.61\sin(8.5)\left(1 - \frac{0.229^2}{0.4451^2}\right)^2 + 0.0202 \times \frac{0.575}{0.33705}$$

$$K = 0.2430$$

Now,

$$h_L = K\frac{V^2}{2g} = 0.2430 \times \frac{(0.18483)^2}{2 \times 9.81}$$

$$\boldsymbol{Minor\ Loss = h_L = 0.0004231\ m}$$

5.2.2. Volume:

By using the trapezoidal formula.

$$Volume = \frac{1}{2}(b_1 + b_2) \times h \times L$$

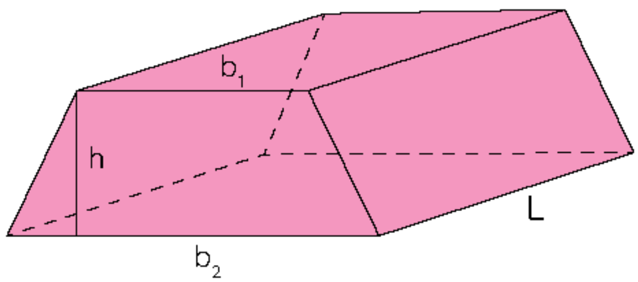

As,

$$b_1 = 229\ mm$$

$$b_2 = 480\ mm$$

$$h = 575\ mm$$

$$L = 430\ mm$$

So,

$$V_1 = \frac{1}{2}(229 + 480) \times 575 \times 430$$

$$V_1 = 87650125\ mm^3$$

And,

$$V_2 = (229 \times 229) \times (110)$$

$$V_2 = 5768510\ mm^3$$

$$V = V_1 + V_2 = 87650125 + 5768510$$

$$\boldsymbol{V = 93418635\ mm^3}$$

$$\boldsymbol{Volume = V = 93.419\ liters}$$

5.3. Baffles:

$$\text{Length of Baffles} = 2\text{ ft} = 36\text{ inch} = 0.610\text{ m}$$

$$Velocity\ in\ Baffles = V_1 = V_2 = V = 0.565375 m/s$$

And,

$$Bafffles\ Dia = D = 0.75\ inch = 0.019\ m$$

$$No. of\ Baffles = n = 229$$

5.3.1. Flow Rate:

$$\mathrm{Q = n \times (A \times V)}$$

$$\mathrm{Q} = 229 \times \frac{\pi}{4}(0.019)^2 \times 0.565375$$

$$\mathbf{Q = 0.0367\ m^3/s}$$

5.3.2. Major Head Loss:

As,

$h_L = \mathrm{f}\frac{L}{D}\frac{V^2}{2g}$…………………......(i)

$$Re = \frac{\mathrm{VD}}{\nu} = \frac{0.565375 \times 0.019}{0.8927 \times 10^{-6}} = 12033.3$$

For Plastic.

$$\Sigma = 0.0015\ mm = 0.0015 \times 10^{-3}\ m$$

So,

$$\frac{1}{\sqrt{f}} = -1.8 \log\left[\left(\frac{0.0015 \times 10^{-3}/_{0.019}}{3.7}\right)^{1.11} + \frac{6.9}{12033.3}\right]$$

$$\frac{1}{\sqrt{f}} = 5.8259$$

$$f = 0.02946$$

Putting the values in eq (i).

$$h_L = 0.02946 \times \frac{0.610}{0.019} \times \frac{(0.565375)^2}{2 \times 9.81}$$

$$\boldsymbol{h_L = 0.00154\ \text{m}}$$

For 229 pipes.

$$h_L = (0.0154) \times 229$$

$$\boldsymbol{Major\ head\ loss = h_L = 0.5287\ m}$$

5.3.3. Volume:

$\text{Number of pipes} = \text{n} = 229$

$\text{Diameter of pipe} = \text{d} = 0.75\ \text{inch}$

$\text{Length of pipe} = \text{l} = 2\ \text{ft} = 24\ \text{inch}$

$\text{Area} = \text{A} = \frac{\pi}{4}(d)^2 = \frac{\pi}{4}(0.75)^2$

$\text{Area} = \text{A} = 0.4418\ inch^2$

$$\text{Volume} = \text{V} = 24 \times 0.4418 \times 229$$

$$\textbf{Volume} = \textbf{V} = \boldsymbol{2428.0584\ inch^3 = 39.789\ litres}$$

5.4. Diffuser:

$\text{Width of diffuser} = W_1 = 9\ \text{inch} = 0.229\ \text{m}$ $\therefore 1 = inlet$

$\text{Width of diffuser} = W_2 = 16.8\ \text{inch} = 0.427\ \text{m}$ $2 = outlet$

$\text{Height of Diffuser} = H_1 = 9\ \text{inch} = 0.229\ \text{m}$

$\text{Height of Diffuser} = H_2 = 18.3\ \text{inch} = 0.465\ \text{m}$

$\text{Length of diffuser} = \text{L} = 22.7\ \text{inch} = 0.575\ \text{m}$

As we know ,

$$V_2 = 0.565375\frac{m}{s} \qquad \therefore Velocity\ at\ Outlet\ of\ diffuser = velocity\ in\ Baffle$$

$$V_1 = \frac{A_2V_2}{A_1} = \frac{(0.465 \times 0.427) \times 0.565375}{(0.229 \times 0.229)}$$

$$\boldsymbol{V_1 = 2.1406\ m/s}$$

5.4.1. Minor Head Loss:

$$Hydraulic\ dia = D_{h1} = 0.229\ m$$

And,

$$Re = \frac{\mathrm{V}D_h}{\nu} = \frac{2.1406 \times 0.229}{0.8927 \times 10^{-6}} = 549117$$

As,

$$D_{h1} = 0.229\ m$$

$$D_{h2} = \frac{2(H_2 \times W_2)}{(H_2 + W_2)} = \frac{2(0.465 \times 0.427)}{(0.465 + 0.427)} = 0.4451\ m$$

For Galvanized iron.

$$\Sigma = 0.15\ mm = 0.15 \times 10^{-3}\ m$$

So,

$$\frac{1}{\sqrt{f_1}} = -1.8\log\left[\left(\frac{0.15 \times 10^{-3}/0.229}{3.7}\right)^{1.11} + \frac{6.9}{549117}\right]$$

$$\frac{1}{\sqrt{f_1}} = 7.3646$$

$$f_1 = 0.01844$$

And,

$$\frac{1}{\sqrt{f_2}} = -1.8\log\left[\left(\frac{0.15 \times 10^{-3}/0.4451}{3.7}\right)^{1.11} + \frac{6.9}{549117}\right]$$

$$\frac{1}{\sqrt{f_2}} = 7.819$$

$$f_2 = 0.0163$$

$$f_{avg} = \frac{f_1 + f_2}{2} = \frac{0.01844 + 0.0163}{2} = 0.01737$$

As,

$$K = 2.61 \sin\theta \left(1 - \frac{{D_{h1}}^2}{{D_{h2}}^2}\right)^2 + f_{avg} \frac{L}{d_{avg}}$$

$$d_{avg} = \frac{0.229 + 0.4451}{2} = 0.33705$$

So,

$$K = 2.61 \sin(6.5) \left(1 - \frac{0.229^2}{0.4451^2}\right)^2 + 0.01737 \times \frac{0.575}{0.33705}$$

$$K = 0.1893$$

Now,

$$h_L = K \frac{V^2}{2g} = 0.1893 \times \frac{(2.1406)^2}{2 \times 9.81}$$

$$\boldsymbol{Minor\ Loss = h_L = 0.04421\ m}$$

5.4.2. Volume:

$$V = V_1 = 87650125\ mm^3$$

$$\boldsymbol{Volume = V = 87.65\ liters}$$

5.5. Pipes:

Length of pipes = L = 3.048 m = 10 ft = 120 inches

Diameter of pipe = d = 0.076 m = 3inch

Kinematic Viscosity = ν = 0.8927×10^{-6}

Flow Rate $= Q = 0.0367 \frac{m^3}{s}$ $\therefore$ *For Velocity in test section*

Area $= A = \frac{\pi}{4}(d)^2 = \frac{\pi}{4}(0.076)^2$

Area $= A = 0.004536\, m^2 = 7.030\, inch^2$

Density of water $= \rho = 998$ kg/m^3

So,

$$Q = A \times V$$

$$V = \frac{Q}{A} = \frac{0.0367}{0.004536} = 8.090\, m/s$$

5.5.1. Major Head Loss:

As,

$h_L = f\frac{L}{D}\frac{V^2}{2g}$……………………......(i)

And,

$$Re = \frac{VD}{\nu} = \frac{8.090 \times 0.076}{0.8927 \times 10^{-6}} = 688742$$

Now for head loss, Using Haaland Equation

$$\frac{1}{\sqrt{f}} = -1.8 \log\left[\left(\frac{\Sigma/_D}{3.7}\right)^{1.11} + \frac{6.9}{Re}\right]$$

For Plastic drawn Tube.

$$\Sigma = 0.0015\, mm = 0.0015 \times 10^{-3}\, m$$

So,

$$\frac{1}{\sqrt{f}} = -1.8 \log\left[\left(\frac{0.0015 \times 10^{-3}/_{0.076}}{3.7}\right)^{1.11} + \frac{6.9}{688742}\right]$$

$$\frac{1}{\sqrt{f}} = 8.8961$$

$$f = 0.0126$$

Putting the values in eq (i).

$$h_L = 0.0126 \times \frac{3.048}{0.076} \times \frac{(8.090)^2}{2 \times 9.81}$$

$$\boldsymbol{Major\ Head\ Loss = h_L = 1.685\ \mathrm{m}}$$

5.5.2. Volume:

$\text{Length of pipes} = \mathrm{L} = 3.048\ \mathrm{m} = 24\ \mathrm{ft} = 288\ \text{inches}$

$\text{Diameter of pipe} = \mathrm{d} = 0.0762\ \mathrm{m} = 3\text{inch}$

$\text{Area} = \mathrm{A} = \frac{\pi}{4}(d)^2 = \frac{\pi}{4}(0.076)^2$

$$\text{Area} = \mathrm{A} = 0.004536\ m^2 = 7.030\ inch^2$$

$$V = A \times L = (7.030) \times 288 = 2024.64\ inch^3$$

$$\boldsymbol{Volume = V = 33.178\ liters}$$

5.6. Design for Water Tank:

Total Volume = $V_{diffuser} + V_{baffle} + V_{nozzle} + V_{test\_section} + V_{pipes}$

$V_T = 87.65 + 39.789 + 93.419 + 47.785 + 33.178$

$V_T = 304.821$ Liters

So, we need a water storage tank that has volume is greater than 301.821 liters. Therefore, with factor of safety we will fabricate/purchase 500 liters water storage tank.

5.7. Bends:

$\text{Diameter of pipe} = \mathrm{d} = 0.076\ \mathrm{m} = 3\text{inch}$

$$\text{Area} = \mathrm{A} = \frac{\pi}{4}(d)^2 = \frac{\pi}{4}(0.076)^2$$

$$\text{Area} = \mathrm{A} = 0.004536\ m^2 = 7.030\ inch^2$$

$\text{Density of water} = \rho = 998\ \mathrm{kg/m^3}$

So,

$$Q = A \times V$$

$$V = \frac{Q}{A} = \frac{0.0367}{0.004536} = 8.090\ m/s$$

5.7.1. Flow Rate:

As we know that,

$$\mathbf{Q = 0.0367\ m^3/s} \qquad \therefore\ For\ Velocity\ in\ test\ section$$

5.7.2. Minor Head Loss:

As,

$$h_L = K\frac{V^2}{2g}$$

$K = 0.2$ $\quad (Long\ Radius\ 90°\ , Flanged)$

$So,$

$$h_L = 0.2 \times \frac{(8.090)^2}{2 \times 9.81}$$

$$\boldsymbol{Minor\ Loss = h_L = 0.667}$$

5.8. Valves:

Diameter of pipe = d = 0.076 m = 3inch

$\text{Area} = \text{A} = \frac{\pi}{4}(d)^2 = \frac{\pi}{4}(0.076)^2$

$\text{Area} = \text{A} = 0.004536\ m^2 = 7.030\ inch^2$

$So,$

$V = \frac{Q}{A} = \frac{0.0367}{0.004536} = 8.090\ m/s$

5.8.1. Flow Rate:

As we know that,

$$\mathbf{Q = 0.0367\ m^3/s} \qquad \therefore\ For\ Velocity\ in\ test\ section$$

5.8.2. Minor Head Loss:

As,

$$h_L = K\frac{V^2}{2g}$$

$$K = 0.15 \qquad (Angle\ , Fully\ Open)$$

$So,$

$$h_L = 0.15 \times \frac{(8.090)^2}{2 \times 9.81}$$

$$\boldsymbol{Minor\ Loss = h_L = 0.5}$$

5.9. Exit Flow Condition at Diffuser (sharp Edge):

5.9.1. Minor Head Loss:

As,

$$h_L = K\frac{V^2}{2g}$$

$K = 2 \qquad (Angle\ , Fully\ Open)$

$V = 2 \qquad (velocity\ we\ \ have\ enter\ /\ diffuser\ inlet\ or\ pipe\ velocity)$

$So,$

$$h_L = 2 \times \frac{(2)^2}{2 \times 9.81}$$

$$\boldsymbol{Minor\ Loss = h_L = 0.2038}$$

5.10. Pump Power:

Density of water = ρ = 998 kg/m^3

g = 9.81 m/s

Total Head Loss in the Water Tunnel = H = 6.4737

Flow Rate of water in the test section at $0.7\frac{\mathrm{m}}{\mathrm{s}} = \mathrm{Q} = 0.0367\ m^3/s$

$So,$

$$Power = P = \rho \times g \times H \times Q$$

$$P = 998 \times 9.81 \times 7.8478 \times 0.0367$$

$\boldsymbol{Required\ Pump\ Power = P = 2819.76\ watt}$ ∴Without Factor of Safety

$Now,$

$\boldsymbol{P^* = P \times \frac{1}{746} = 2819.76 \times \frac{1}{746} = 3.77\ hp}$ (Without Factor of Safety)

$\boldsymbol{Required\ Power = P^* = 3.77 \times 1.5 = 5.66\ hp}$ (With Factor of Safety)

5.11. Total Head Losses:

Velocity = 0.7 m/s **Flow rate = 0.0367 m^3/s**	
Component	**Head Losses**
BAFFLES	3.52 m
NOZZLE	0.00042 m
DIFFUSER	0.0442 m
TEST SECTION	0.00158 m
SUDDEN EXPANSION	0.2038
PIPE 3in	1.6912 m
4x 90^0 bend 3in	0.6674 m
Gate Valve	0.5 m
Suction Head	1.2192 m

Total Head Loss(m)	**7. 8478 m**

TABLE 5-1 TOTAL HEAD LOSS DETERMINED

5.12. Pump Selection:

Flow Rate	0.0367 m^3/s
Required Flow Rate	**2172 LPM**
Total Head losses	7.8478 m
Power (without factor of safety)	3. 77 hp
Power (factor of safety= 1.5)	5.66 hp
5hp Pump Flow Rate=	505 LPM
10hp Pump Flow Rate	**2200 LPM**

TABLE 5-2 PUMP SELECTION TABLE

10 hp Pump it was selected.

(1 gallon per hour = 0.06309 liters per minute)

Chapter 6 Verification of Calculations from MATLAB Codes:

The Calculations of the Minor and Major Head losses were verified by using the following MATLAB codes. The purpose of the code was to change multiple variables like (Cross-Sectional area, Diameter of pipe and no. of pipes) to get desirable results.

6.1. Test Section:

```
disp('All the calculations are in SI Unit')
disp('TEST SECTION')
W=0.229;                                 % 9 inch
H=0.229;                                 % 9 inch
Dh=(2*H*W)/(H+W);
A= W*H;
fprintf('Area is = %d m^2 \n',A);
L=0.9144;                                % 3 feet
V=0.7;
Q=A*V;                                   %At V=0.7 m/s
fprintf('Flow rate is = %d m^3/s \n',Q);
v=0.8927*10^-6;      % kinematic viscocity at 30 degree centigrade of water
Re=V*Dh/v;
fprintf('Reynold Number is = %g \n',Re);
E=0.0015*10^-3;                          %Plastic drawn tube roughness
f = (1/(-1.8*log10((6.9/Re)+(E/Dh/3.7)^1.11)))^2; % Haaland Equation
fprintf('Co-efficient of friction is = %d \n',A);
h_major= (f*L*V^2)/(Dh*2*9.81);
fprintf('Major Head Loss is = %f m \n',h_major);
```

FIGURE 6-1 MATLAB CODE FOR DETERMINING MAJOR HEAD LOSS IN TEST SECTION

```
All the calculations are in SI Unit
TEST SECTION
Area is = 5.244100e-02 m^2
Flow rate is = 3.670870e-02 m^3/s
Reynold Number is = 179568
Co-efficient of friction is = 5.244100e-02
Major Head Loss is = 0.001582 m
```

FIGURE 6-2 RESULTS OF MAJOR HEAD LOSS IN TEST SECTION

6.2. Nozzle:

```
disp('All the calculations are in SI Unit')
disp('NOZZLE')
W1=0.427;
H1=0.465;
W2=0.229;
H2=0.229;
Q = 3.670870e-02;                   % contant flow rate in the water tunnel
fprintf('Flow rate is = %d m^3/s \n',Q);
Dh1=(2*H1*W1)/(H1+W1);
Dh2=(2*H2*W2)/(H2+W2);
Dhav=(Dh1+Dh2)/2;
fprintf('Average Hydraulic Diameter is = %d m \n',Dhav);
L=0.575;
theta=8.5;
A1=W1*H1;
A2=W2*H2;
V1=Q/A1;
fprintf('Velocity at the inlet of nozzel is = %g m/s \n',V1);
v=0.8927*10^-6;       % kinematic viscocity at 30 degree centigrade of water
Re=V1*Dh1/v;
fprintf('Reynold Number is = %g \n',Re);
E=0.15*10^-3;                        % Galvanized Iron roughness
f1 = (1/(-1.8*log10((6.9/Re)+(E/Dh1/3.7)^1.11)))^2; % Haaland Equation
f2 = (1/(-1.8*log10((6.9/Re)+(E/Dh2/3.7)^1.11)))^2;
fav=(f1+f2)/2;
fprintf('Average Co-efficient of Friction is = %d \n',fav);
K=2.61*sind(theta)*(1-(Dh2/Dh1)^2)^2+fav*(L/Dhav);
fprintf('Minor loss Co-efficient is = %d \n',K);
h_minor= (K*V1^2)/(2*9.81);
fprintf('Minor Head Loss is = %f m \n',h_minor);
```

FIGURE 6-3 MATLAB CODE FOR DETERMINING MINOR HEAD LOSS IN NOZZLE

```
All the calculations are in SI Unit
NOZZLE
Flow rate is = 3.670870e-02 m^3/s
Average Hydraulic Diameter is = 3.370953e-01 m
Velocity at the inlet of nozzel is = 0.184879 m/s
Reynold Number is = 92199.5
Average Co-efficient of Friction is = 2.024441e-02
Minor loss Co-efficient is = 2.431719e-01
Minor Head Loss is = 0.000424 m
```

FIGURE 6-4 RESULTS OF MINOR HEAD LOSS IN NOZZLE

6.3. Baffles:

```
disp('All the calculations are in SI Unit')
disp('BAFFLES')
D=0.019;                          % 0.75 inch Pipe used
L=0.610;                          % 2 feet Baffle length
n=229;
fprintf('Total Number of Pipes in Baffle is = %d \n',n);
Q = 3.670870e-02;                 % contant flow rate in the water tunnel
fprintf('Flow rate is = %d m^3/s \n',Q);
A1 = n*((pi/4)*(D.^2));           % A1=A2
V1 = Q/A1;                        %velocity in baffle pipes V1=V2
fprintf('Velocity in baffles = %g m/s \n',V1);
v=0.8927*10^-6;       % kinematic viscocity at 30 degree centigrade of water
Re=(V1*D)/v;
fprintf('Reynold Number is = %g \n',Re);
E=0.0015*10^-3;                   %Plastic drawn tube roughness
f=(1/(-1.8*log10((6.9/Re)+(E/D/3.7)^1.11)))^2;  % Haaland Equation
fprintf('Co-efficient of Friction is = %d \n',f);
h_major= (f*L*V1^2)/(D*2*9.81);
totalh_major= n*h_major;
fprintf('Total Major Head Loss in Baffles is = %f m \n',totalh_major);
```

Figure 6-5 MATLAB code for determining major head loss in baffles

```
All the calculations are in SI Unit
BAFFLES
Total Number of Pipes in Baffle is = 229
Flow rate is = 3.670870e-02 m^3/s
Velocity in baffles = 0.565375 m/s
Reynold Number is = 12033.3
Co-efficient of Friction is = 2.946276e-02
Total Major Head Loss in Baffles is = 3.529060 m
```

Figure 6-6 Results of major head loss in baffles

6.4. Diffuser:

```
disp('All the calculations are in SI Unit')
disp('Diffuser')
W1=0.229;
H1=0.229;
W2=0.427;
H2=0.465;
Dh1=0.229;
Dh2=(2*(H2*W2))/(H2+W2);
Dhav=(Dh1+Dh2)/2;
fprintf('Average Hydrualic Diameter = %d m \n',Dhav);
L=0.575;
theta=6.5;
A1=W1*H1;
A2=W2*H2;
V2=0.565375;    % velocity in the baffle = velocity at the exit of diffuser
V1=(A2/A1)*V2;
v=0.8927*10^-6; % kinematic viscocity at 30 degree centigrade of water
Re=V1*Dh1/v;
fprintf('Reynold Number is = %g \n',Re);
E=0.15*10^-3;   % Galvanized Iron roughness
f1 = (1/(-1.8*log10((6.9/Re)+(E/Dh1/3.7)^1.11)))^2; % Haaland Equation
f2 = (1/(-1.8*log10((6.9/Re)+(E/Dh2/3.7)^1.11)))^2;
fav=(f1+f2)/2;
fprintf('Average Co-efficient of Friction is = %d \n',fav);
K=2.61*sind(theta)*(1-(Dh1/Dh2)^2)^2+fav*(L/Dhav);
fprintf('Minor Loss Co-efficient is = %d \n',K);
h_minor= (K*V1^2)/(2*9.81);
fprintf('Minor Loss is = %f m \n',h_minor);
```

FIGURE 6-7 MATLAB CODE FOR DETERMINING MAJOR HEAD LOSS IN DIFFUSER

```
All the calculations are in SI Unit
Diffuser
Average Hydrualic Diameter = 3.370953e-01 m
Reynold Number is = 549132
Average Co-efficient of Friction is = 1.739663e-02
Minor Loss Co-efficient is = 1.894660e-01
Minor Loss is = 0.044251 m
```

FIGURE 6-8 RESULTS OF MINOR HEAD LOSS IN DIFFUSER

6.5. Pipes:

```
disp('All the calculations are in SI Unit')
disp('Major loss')
%L = input('Enter length of pipe = ');
L=3.048;
D = 0.076;             % For 3 inch diameter of pipe
Q=3.670870e-02;         % For velocity in the test section = 0.7 m/s
A=(pi/4)*D^2;
V = Q/A;
v = 0.8927*10^-6;       % kinematic viscocity at 30 degree centigrade of water
density = 998;
E=0.0015*10^-3;         %Plastic drawn tube roughness;
g = 9.81;
Re =(V*D)/v;
fprintf('reynold number = %0.4f unit less \n',Re)
if (Re < 2300);
    f = 64/Re;
    fprintf('reynold <2300) flow is laminar so f = %0.4f unit less\n',f);
else (Re > 2300);
    disp('reynold>2300 so flow is turbulent');
    f=(1/(-1.8*log10((6.9/Re)+(E/D/3.7)^1.11)))^2;  % Haaland Equation
    fprintf ('Co-efficient of friction of pipe is = %0.4f unitless\n',f);
end
h_major = f*(L/D)*(V.^2/(2*g));
fprintf('Major Head loss is = %0.4f m \n',h_major)
```

FIGURE 6-9 MATLAB CODE FOR DETERMINING MAJOR HEAD LOSSES IN PIPES

```
All the calculations are in SI Unit
Major loss
reynold number = 688906.0461 unit less
reynold>2300 so flow is turbulent
Co-efficient of friction of pipe is = 0.0126 unitless
Major Head loss is = 1.6912 m
```

FIGURE 6-7 RESULT OF MAJOR HEAD LOSS IN PIPES

6.6. Bends:

```
clc
clear all
close all
disp('All the calculations are in SI Unit')
disp('Bends')
Q=3.670870e-02;        % Flow are at 0.7 m/s velocity in test section
D = 0.076;             % 3 inches diameter
A=(pi/4)*D^2;
V = Q/A;
KL= 0.2;               %Long radus 90 degree, flanged
g = 9.81;
h_minor= (KL*V^2)/(2*g);
fprintf('Minor Head Loss is = %f m \n',h_minor);
```

FIGURE 6-11 MATLAB CODE FOR DETERMINING MINOR HEAD LOSS IN BENDS

```
All the calculations are in SI Unit
Bends
Minor Head Loss is = 0.667475 m
```

Published with MATLAB® R2017b

FIGURE 6-8 RESULTS OF MINOR HEAD LOSS IN BENDS

6.7. Valves:

```
clc
clear all
close all
disp('All the calculations are in SI Unit')
disp('Vavle')
Q=3.670870e-02;       % Flow are at 0.7 m/s velocity in test section
D = 0.076;            % 3 inches diameter
A=(pi/4)*D^2;
V = Q/A;
KL= 0.15;              %gate, fully open
g = 9.81;
h_minor= (KL*V^2)/(2*g);
fprintf('Minor Head Loss is = %f m \n',h_minor);
```

```
All the calculations are in SI Unit
Vavle
Minor Head Loss is = 0.500606 m
```

FIGURE 6-9 MATLAB CODE FOR DETERMINING MINOR HEAD LOSS IN VALVES AND RESULTS

6.8. Pump Power:

```
clc;
close all;
clear all;
disp('All the calculations are in SI Unit')
disp('Pump Power')
density = 998;
g = 9.81;
%H = input('Enter the total Head loss = ');% Total Head loss in the water tunnel
H = 7.8478
Q = 3.670870e-02;    % Flow rate of water in the test section at 0.7 m/s
P = density*g*H*Q;
fprintf('The Required Pump Power Without Factor of Safety = %f Watt \n',P);
h = P*(1/746);
fprintf('The Required Pump Power Without Factor of Safety = %f hp \n',h);
```

FIGURE 6-10 MATLAB CODE TO DETERMINE PUMP POWER

```
All the calculations are in SI Unit
Pump Power
The Required Pump Power Without Factor of Safety = 2819.48 2 Watt
The Required Pump Power Without Factor of Safety = 3.77 hp
```

Published with MATLAB® R2017b

FIGURE 6-11 RESULTS OF DETERMINING PUMP POWER

Chapter 7 Fabrication

All the fabrication was done under the premises of university, and the fabrication processes were performed under the supervision of competent authority using in-house materials.

7.1. Diffuser:

The cross-section of the diffuser inlet and exit according to our design is 230 mm by 230 mm and 480mm by 430 mm, respectively. The length of the diffuser is kept at 575mm. The main purpose of the diffuser is to reduce the velocity of the water. We have used galvanized sheets for the manufacturing of it. The benefit of that is it gives too much strength against the pressure of water which will hold inside it during the experimentation. The galvanized sheets have a high resistance to corrosion, which will consequently increase the life span of the apparatus. The thickness of the sheet is 1.5mm and it is lighter in weight as compared to the ordinary iron sheets. We have used the iron frame at the entrance and exit of the diffuser which helps with the proper support to make the diffusers shaped to be built.

7.2. Baffle:

The cross-section of the baffle is 480mm by 430mm. An angle iron is used on all four sides of the baffle frame. These angle irons are welded by a square cross-section plate frame on both sides. The baffle is put in such a way that all the water coming from the diffuser enters the pipes and exits from the pipes to the nozzle section. To make sure the water flows within the pipes, the gap between the pipes has been blocked by a thin layer of cement. The purpose of using a baffle is to eliminate the longitudinal turbulence present in the flow. So, this would only be possible if all the water flowed within the pipes. The diameter of the pipes used in the baffle is 19mm. The pipes are Polyvinyl chloride pipes (PVC pipes). The top and bottom of the baffles are closed with an iron plate. A drain is drilled at the bottom of the baffle plate. Wire meshes at the entrance and at the exit of the baffle.

FIGURE 7-1 FABRICATION PROCEDURE OF BAFFLES

7.3. Test Section Inlet Nozzle:

The cross-section of the nozzle inlet is 430 x 480 mm and for outlet 230 x 230 mm, respectively. The length of the nozzle is kept at 685mm. Galvanized sheets are used because of their high resistance to corrosion. The thickness of the sheet is 1.5mm. An iron frame at the entrance and exit of the nozzle which helps in the proper support to make the nozzle’s shape be built. At the exit side of the nozzle,110mm length of the nozzle has no change in the cross-section, because the flow of water abruptly going from the nozzle to the test section will cause the flow disturbance. Which will finally affect the results during the experimentations.

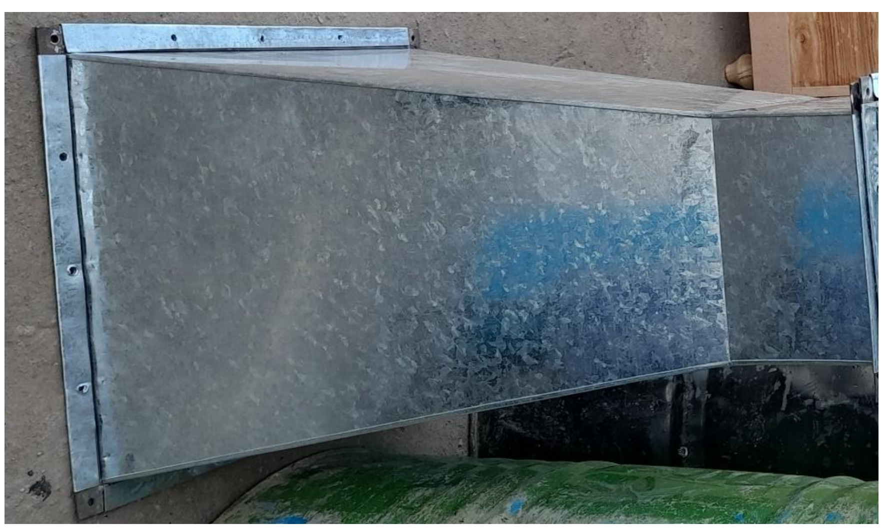

FIGURE 7-2 FABRICATION OF NOZZLE

7.4. Test Section:

The cross-section of the test section is 9 x 9 inches. Angle iron is used for all sides of the to reinforce the structure. Instead of using glass, acrylic sheets used for the test section. The benefit of its usage is that acrylic sheets have an extremely high impact strength. The sheets are joined and sealed by using hardener epoxy. A slot was cut at the top layer to place the test specimen or for dye injection.

FIGURE 7-3 FABRICATION STEPS OF TEST SECTION

Silicone gel has been used to join the acrylic sheet together. For the leakage factor safety purpose, we have also added Epoxy Glue over it. The procedure of putting Epoxy Glue is that; we first mix the Epoxy Glue Resin (Part-A) with Epoxy Glue Hardener (Part-B) and heat that up while mixing. The purpose of heating is to thoroughly mix the two parts. After completely mixing we have put the mixture over the joints.

FIGURE 7-4 EPOXY RESIN USED FOR LEAKAGE (HARDENER)

7.5. Test Section Exit Nozzle:

After the test section, sudden contraction will cause a backflow which will disturb the flow phenomenon in the test section and the studies on the model in the test section will be disturbed. So, to avoid that situation an exit nozzle is designed, which will gradually contact the test section area and channel the water into a 100mm diameter pipe.

FIGURE 7-5 TRANSITION NOZZLES

7.6. Plumbing System:

Standard PVC pipes are used overall. The exit of the pump is 2 inches in diameter. A union is used which expands to 3 inches. The socket is used which helps to install the Ball Valve. The valve helps in controlling the flow in the water tunnel. With this, multiple experiments at different velocities can be performed in the test section. Also, the piping system is connected to a flexible pipe to absorb all the vibrations and transfer the water to the water tunnel inlet.

FIGURE 7-6 PLUMBING SUBSYSTEM

7.7. Pump Installation:

To meet the maximum required flow i.e., 0.7m/s in the test section a centrifugal pump of 10 HP was purchased. It has backward curved blades with 3470 RPM, 2133 FR. The model is LVA 213TTDW7303AB. It operates on both two-phases and three-phases i.e., 220/380 Volt supported with 60 Hz. The pump is fixed on iron stand which is bolted on the ground to reduce the vibration caused during its work.

FIGURE 7-7 10 HP PUMP

7.8. Water Storage reservoir:

By calculating the volume of all the components of the water tunnel i.e., diffuser, baffle, nozzle, test section, and the plumbing g subsystem, add to 320 liters. So, the minimum water storage reservoir is 320 liters. However, to avoid overflow an 800-liter water storage reservoir is used.

FIGURE 7-8 WATER RESERVOIR

Chapter 8 Experimental Setup:

A 4 x 10 Tube Bundle is placed in a low-speed water tunnel. (Fig.8.1) The model contains 40 rods in cross-arrangement and a cross arrangement having 40 Tubes. Each Tube has a length of 120 mm, outer diameter of 12mm, inner diameter of 11.5 mm, and a pitch of 18.56 mm. Placed in a test section of 260 mm x 270 mm. The Flexible Tube has is suspended by a piano string. And the diameter of hole for flexible tube is 20 mm to accommodate the translational vibration for data measurement. All tubes are rigid accept the flexible tube.

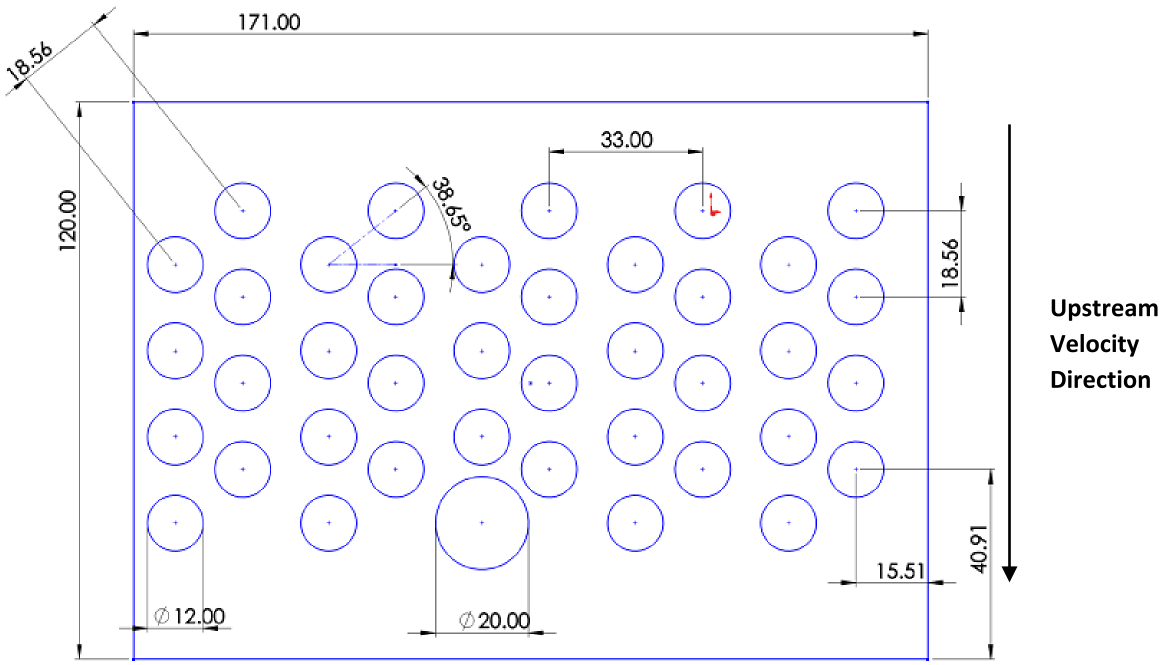

FIGURE 8-1 TRIANGULAR PARALLEL ARRAYS TUBE BUNDLE SPACER PLATE DIMENSIONS

The Experiment performed for a single flexible tube that was fixed in the middle of the last row for all experiments from upstream side of the Tube Bundle. The flexible tube was held by piano wire, and a 1.5 mm hole was drilled at top and bottom to suspend the flexible tube and the piano wires' ends were tied to two acrylic sheets held by nut and bolt. The stiffness of the string was controlled by tightening or loosening the bolt to the desired value. And the Accelerometer (WSDA- Base Station) was used for Vibrational Data Measurement. The acceleration signal is measured at 5 velocities from 0.1 m/s to 0.5 m/s.

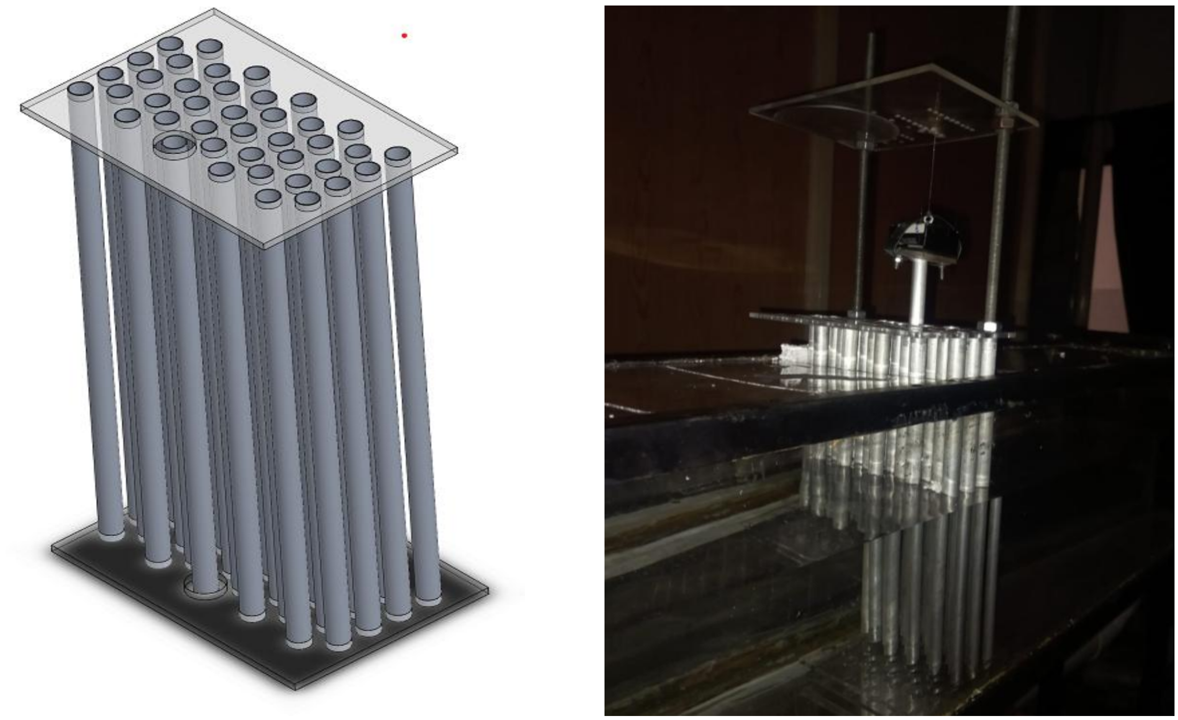

FIGURE 8-1 TUBE BUNDLE MODEL VIEW(LEFT) AND EXPERIMENTAL SETUP(RIGHT)

The Node Commander was used to channel the measurement data from accelerometer to Computer. Then by Sigview the data was interpreted into 3 channels where Channel 2 shows the Transverse amplitude (drag) of the vibration, and Channel 1 shows the Streamwise amplitude (lift) of the vibration.

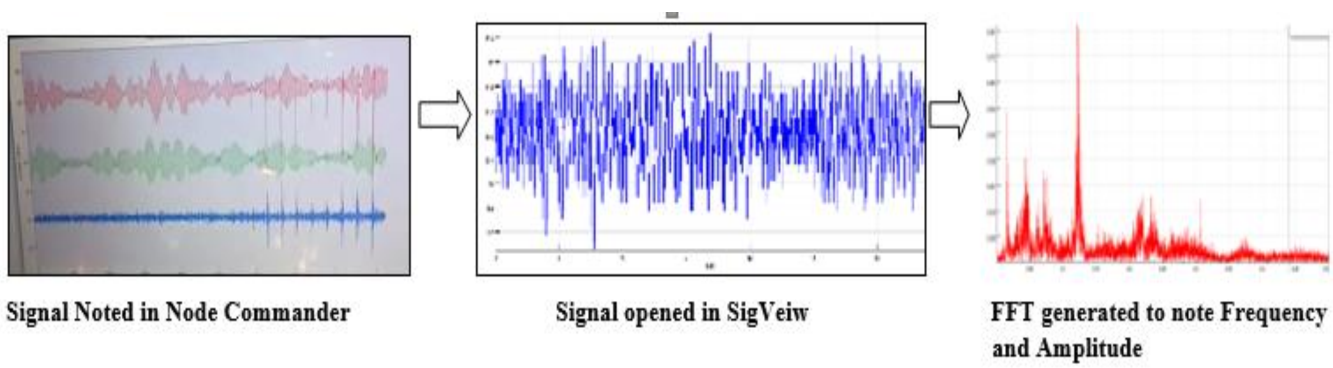

FIGURE 8-2 DATA INTERPRETATION LOOP

The Accelerometer is mounted on the flexible tube in the middle of the last row from the upstream side of the Tube Bundle to measure the flow induced vibrations. The test tube and sensor are suspended by a piano wire from top and bottom, Stiffness of the test tube is adjusted to achieve the natural frequency of 10 Hz, to accurately mimic the surroundings of Shell and Tube Heat exchanger. The Bump Test was performed to measure the natural frequency of the flexible tube. And was adjusted by tightening or loosening the piano wire to reach the desired value of natural frequency of approx. 10 Hz.

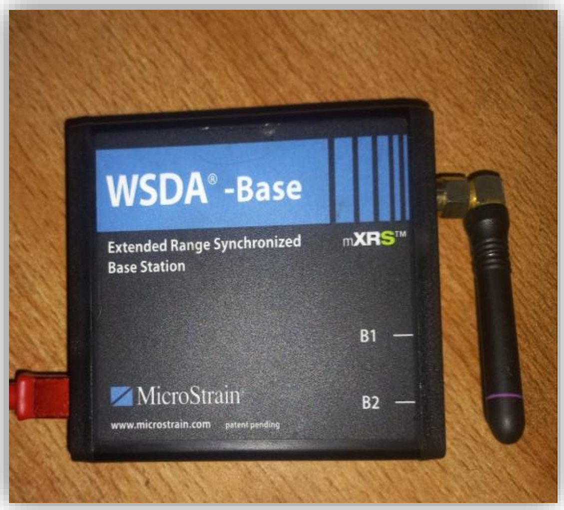

FIGURE 8-3 ACCELEROMETER(LEFT) AND THE SENSOR MOUNTED ON TOP OF THE TUBE BUNDLE (RIGHT)

The monitored tube remained fixed throughout all experiment, but the Number of rows were deducted one by one after conducting every 4 experiments (Varying Factor A), and the response was measured as a function of Reduced Velocity.

20 experiments were recorded by changing the following Factors:

Factor A: Angle of valve to control flow rate (18^0, 36^0, 54^0, 72^0 and 90^0)

Factor B: By removing a single row consecutively from the Tube Bundle

5 valve settings × 4 row configurations = 20 experiments.

8.1. Simulation:

2D Simulation was performed on ANSYS 16.2 through FLUENT for the phenomenon of flow induced vibration. The geometry of the 2D view was made on Ansys at 0 thickness and then a fine Mesh was generated having 1 cm element size, Mesh is adjusted for Method, Sizing, and Inflation. Mesh contains 9040 Nodes and 6601 elements.

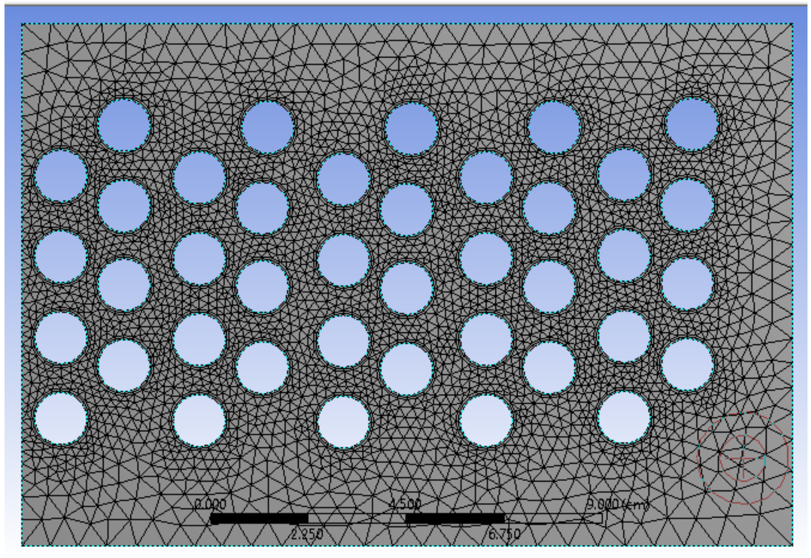

FIGURE 8-4 MESH PREVIEW ON 2D TUBE BUNDLE

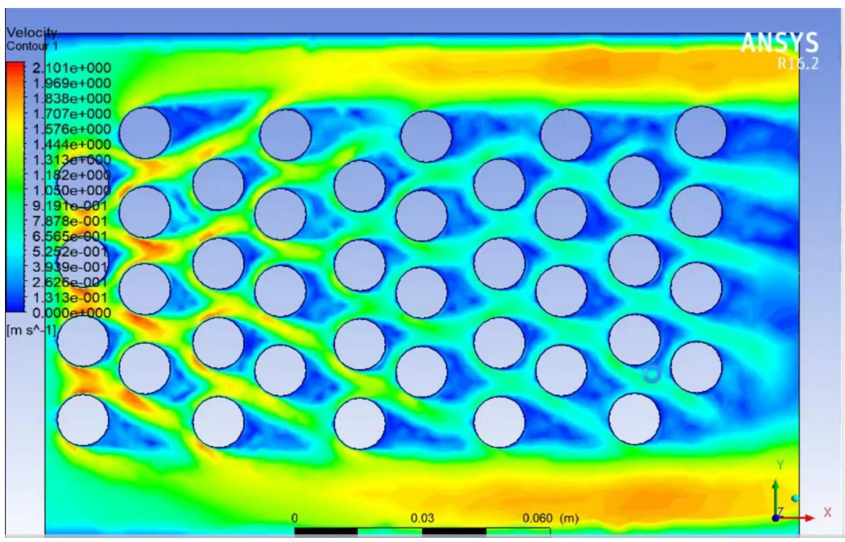

FIGURE 8-5 2D SIMULATION PREVIEW OF TUBE BUNDLE

8.2. Validation:

For the Validation of the Water Tunnel A 4 x 10 Tube Bundle has been experimented upon, the reason for picking this specimen was due to its significance with Shell and Tube Heat Exchangers and their importance in the Process Industry and in nuclear power plants as well. The Tube Bundle used has a Pitch ratio (Pr) of 1.54 according to the literature [45] where Akram et al. studied the effect of flow induced vibrations response on triangular arranged array.

Similarly, our experiment also uses the Pitch ratio of 1.54 for the triangular parallel arrangement array to study the effect of flow induced vibrations at varying flowrates to measure the Reduced Velocity and vibration amplitude.

The Experiment performed for a single flexible tube that was fixed in the middle of the last row for all experiments from upstream side of the Tube Bundle. The flexible tube was held by piano wire, and a 2 mm hole was drilled at top and bottom to suspend the flexible tube and the piano wires' ends were tied to two acrylic sheets held by nut and bolt. The stiffness of the string was controlled by tightening or loosening the bolt to the desired value. And the Accelerometer (WSDA-Base Station) was used for Vibrational Data Measurement. The acceleration signal is measured at 5 velocities from 0.1 m/s to 0.5 m/s.

After the experimentation, the similarities noted are as follows:

- All similarities are taken from single flexible tube experiments.
- The Instability was observed both in streamwise and transverse direction in all four rows, but highest value was recorded in the 3rd row. Moreover, in the third row an early instability is propagated, on the flexible tube specifically in transverse amplitude of vibration.

Chapter 9 Observations:

Axis and Channel No's:
X-axis: Channel 2 (Red)
Y-axis: Channel 1 (Green)
Z-axis: Channel 3 (Blue)

- **Channel 2 shows the drag force values.**
- **Channel 1 shows the lift force values**

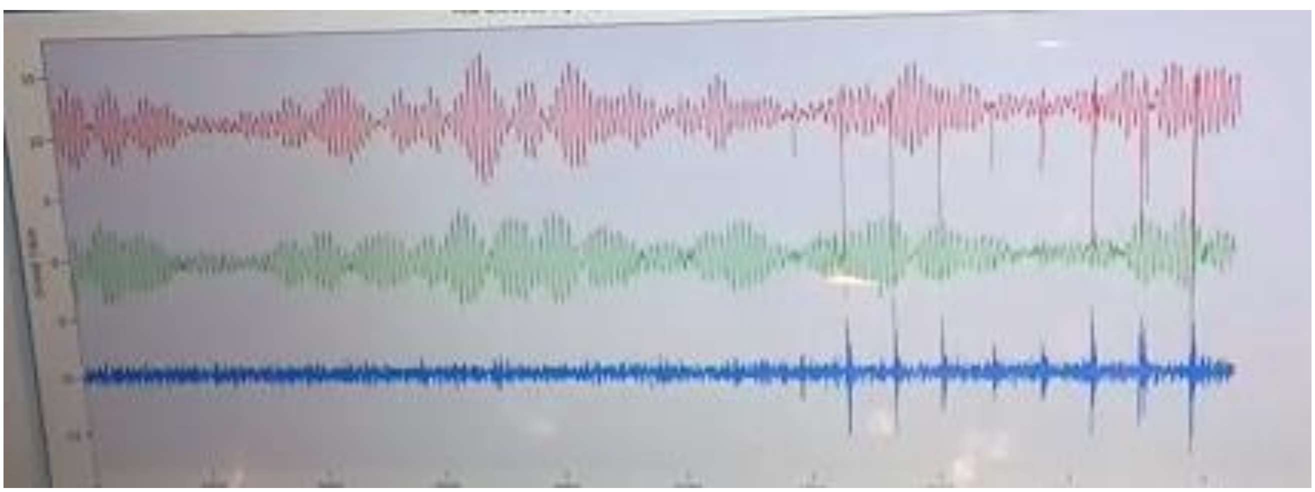

FIGURE 9-1 DIPLAY OF NODE COMMANDER DURING DATA AQUISITION

9.1. Row 1:

Sr. No.	Free Stream Velocity (m/s)	Gap Velocity (m/s)	Reduced Gap Velocity	Streamwise Amplitude (m/s^2)	Transverse Amplitude (m/s^2)	Streamwise Amplitude (% do)	Transverse Amplitude (% do)	Resultant Amplitude (%do)	Damping Ratio	Damping Ratio (%)	Log. Decrement	Mass Damping Parameter
18	0.10	0.16	1.40	0.252	0.289	0.42	0.48	0.64	0.003	0.318	0.020	0.023
36	0.20	0.32	2.80	0.436	0.484	0.73	0.81	1.09	0.005	0.483	0.030	0.035
54	0.30	0.48	4.20	0.534	0.462	0.89	0.77	1.18	0.008	0.812	0.051	0.059
72	0.40	0.64	5.60	0.547	0.550	0.91	0.92	1.29	0.005	0.487	0.031	0.035
90	0.50	0.80	7.00	0.534	0.532	0.89	0.89	1.26	0.005	0.484	0.030	0.035

9.2. Row 2:

Sr. No.	Free Stream Velocity (m/s)	Gap Velocity (m/s)	Reduced Gap Velocity	Streamwise Amplitude (m/s^2)	Transverse Amplitude (m/s^2)	Streamwise Amplitude (% do)	Transverse Amplitude (% do)	Resultant Amplitude (%do)	Damping Ratio	Damping Ratio (%)	Log. Decrement	Mass Damping Parameter
18	0.10	0.16	1.15	0.264	0.288	0.44	0.48	0.65	0.003	0.295	0.019	0.021
36	0.20	0.32	2.30	0.414	0.446	0.69	0.74	1.01	0.005	0.457	0.029	0.033
54	0.30	0.48	3.45	0.633	0.498	1.06	0.83	1.34	0.005	0.460	0.029	0.033
72	0.40	0.64	4.61	0.843	0.663	1.41	1.11	1.79	0.006	0.600	0.038	0.043
90	0.50	0.80	5.76	0.705	0.503	1.18	0.84	1.44	0.005	0.454	0.029	0.033

9.3. Row 3:

Sr. No.	Free Stream Velocity (m/s)	Gap Velocity (m/s)	Reduced Gap Velocity	Streamwise Amplitude (m/s^2)	Transverse Amplitude (m/s^2)	Streamwise Amplitude (% do)	Transverse Amplitude (% do)	Resultant Amplitude (%do)	Damping Ratio	Damping Ratio (%)	Log. Decrement	Mass Damping Parameter
18	0.10	0.16	1.15	0.257	0.213	0.43	0.36	0.56	0.006	0.550	0.035	0.040
36	0.20	0.32	2.30	0.525	0.573	0.88	0.96	1.30	0.004	0.350	0.022	0.025
54	0.30	0.48	3.45	0.856	0.691	1.43	1.15	1.83	0.004	0.004	0.027	0.031
72	0.40	0.64	4.61	0.780	0.674	1.30	1.12	1.72	0.004	0.421	0.026	0.030
90	0.50	0.80	5.76	1.015	0.961	1.69	1.60	2.33	0.003	0.282	0.018	0.020

9.4. Row 4:

Sr. No.	Free Stream Velocity (m/s)	Gap Velocity (m/s)	Reduced Gap Velocity	Streamwise Amplitude (m/s^2)	Transverse Amplitude (m/s^2)	Streamwise Amplitude (% do)	Transverse Amplitude (% do)	Resultant Amplitude (%do)	Damping Ratio	Damping Ratio (%)	Log. Decrement	Mass Damping Parameter
18	0.10	0.16	1.15	0.318	0.380	0.53	0.63	0.83	0.006	0.617	0.039	0.045
36	0.20	0.32	2.30	0.443	0.427	0.74	0.71	1.02	0.008	0.776	0.049	0.056
54	0.30	0.48	3.45	0.566	0.525	0.94	0.87	1.29	0.005	0.474	0.030	0.034
72	0.40	0.64	4.61	0.604	0.514	1.01	0.86	1.32	0.003	0.312	0.020	0.023
90	0.50	0.80	5.76	0.538	0.465	0.90	0.78	1.19	0.005	0.471	0.030	0.034

Chapter 10 Results:

After Splitting the Flow induced Vibration into Transverse and Streamwise Vibrational Amplitude, Reduced Velocity is our unit of measure and comparing the data on all four rows.

10.1. Row 1:

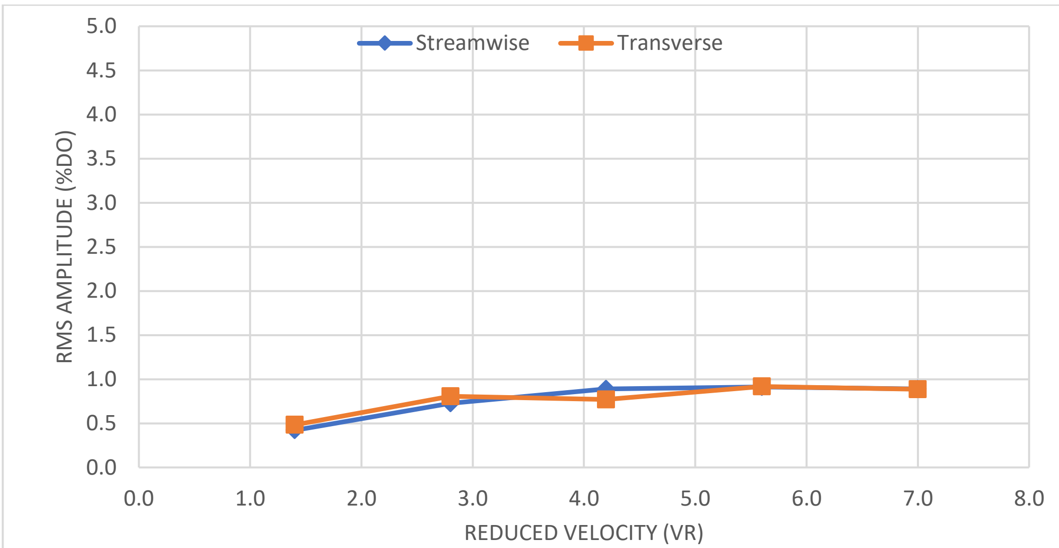

GRAPH 10.1: LIFT AND DRAG AMPLITUDE

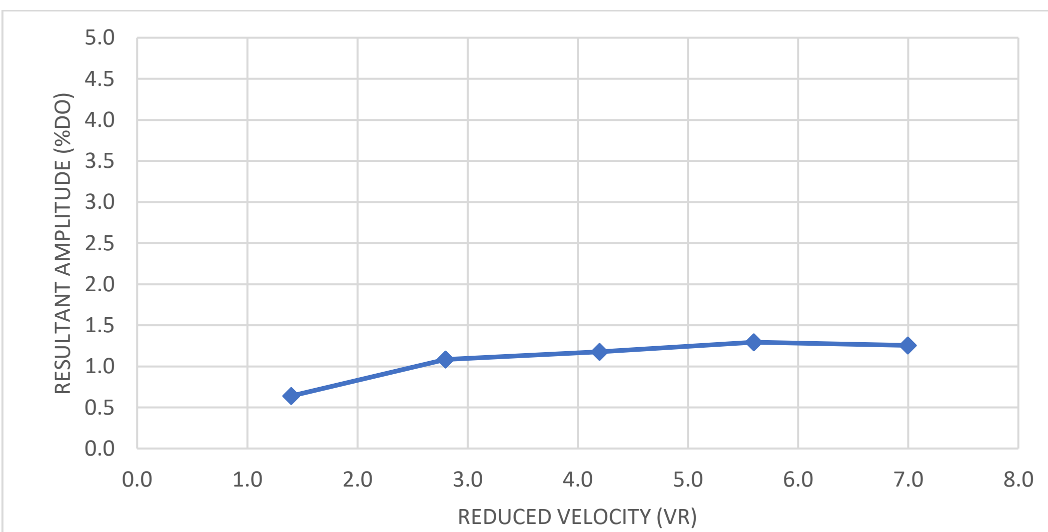

GRAPH 10.2: RESULTANT AMPLITUDE

10.2. Row 2:

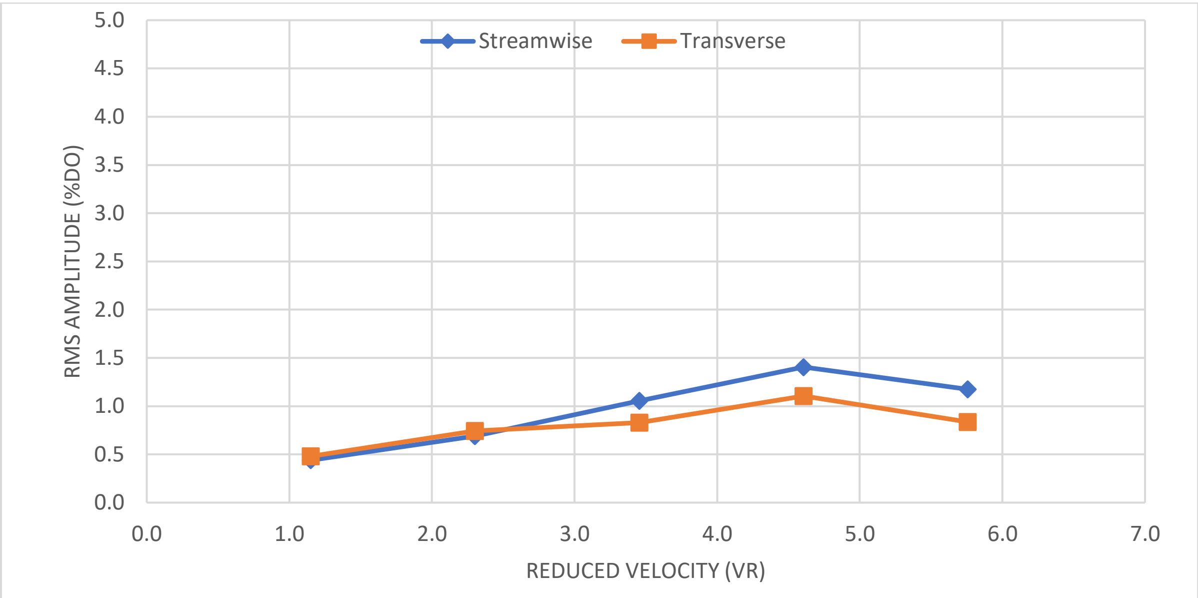

GRAPH 10.3: LIFT AND DRAG AMPLITUDE

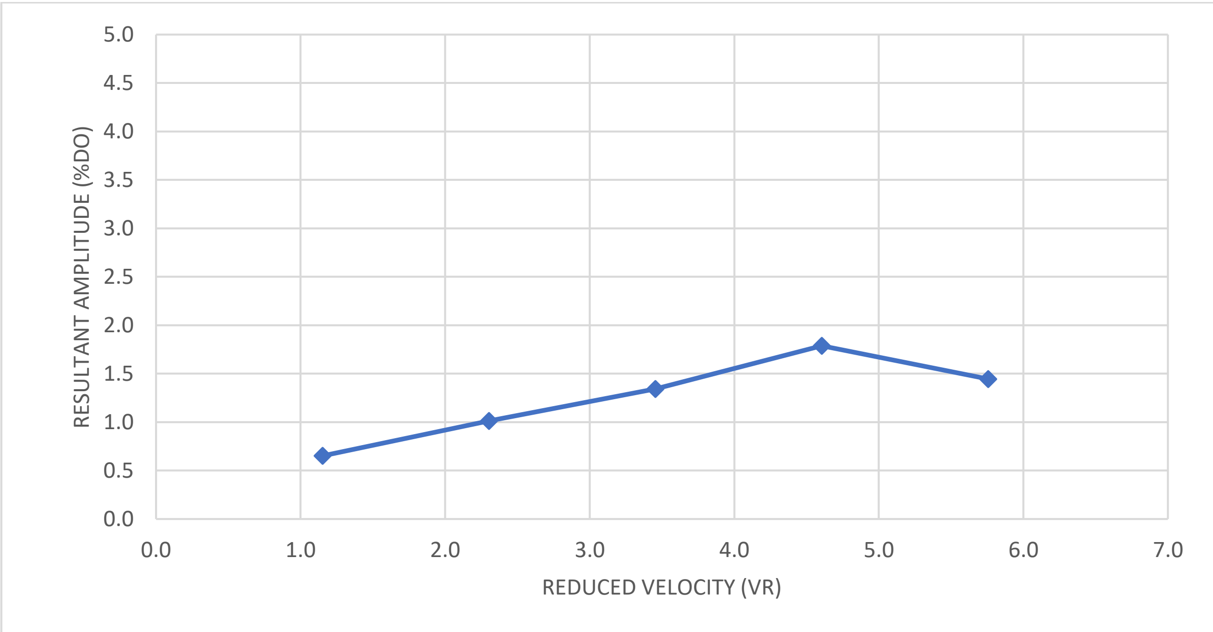

GRAPH 10.4: RESULTANT AMPLITUDE

10.3. Row 3:

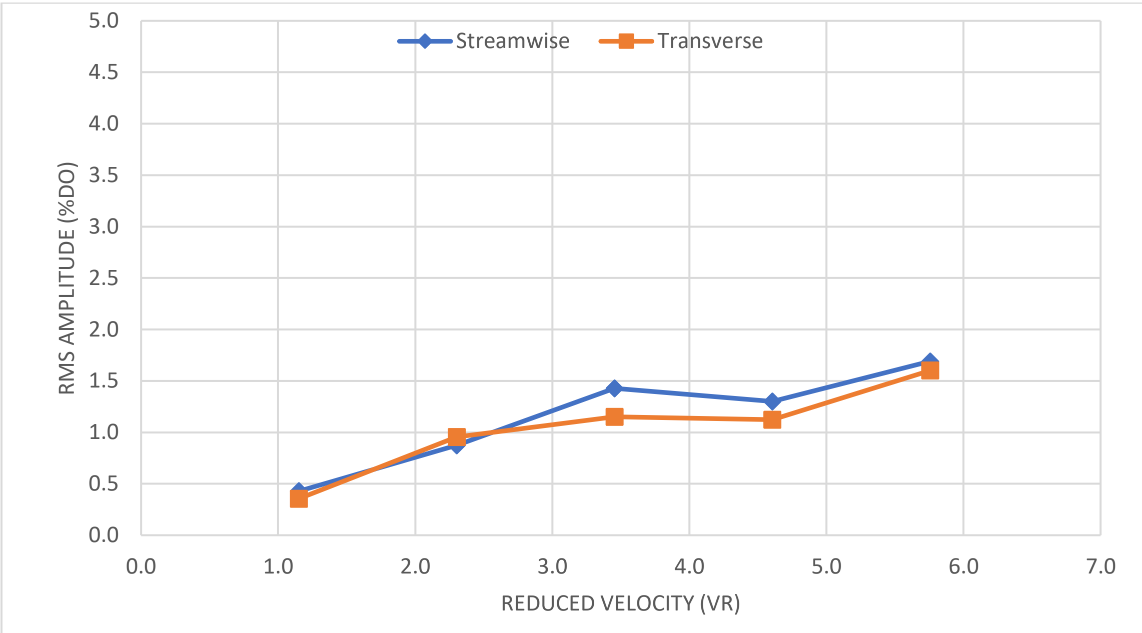

GRAPH 10.5: LIFT AND DRAG AMPLITUDE

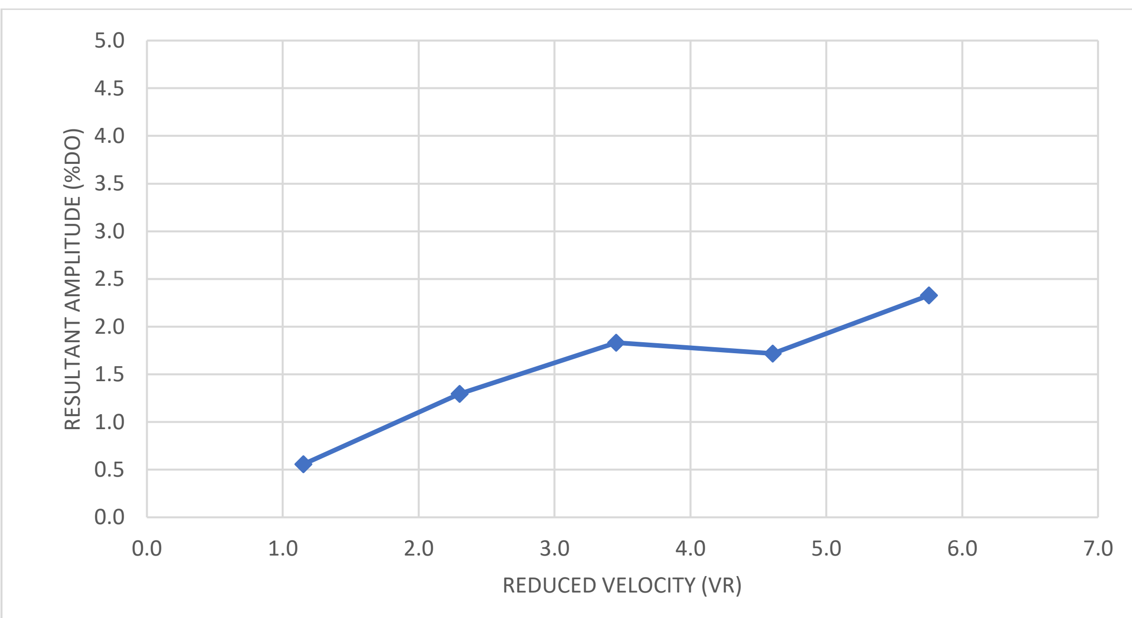

GRAPH 10.6: RESULTANT AMPLITUDE

10.4. Row 4:

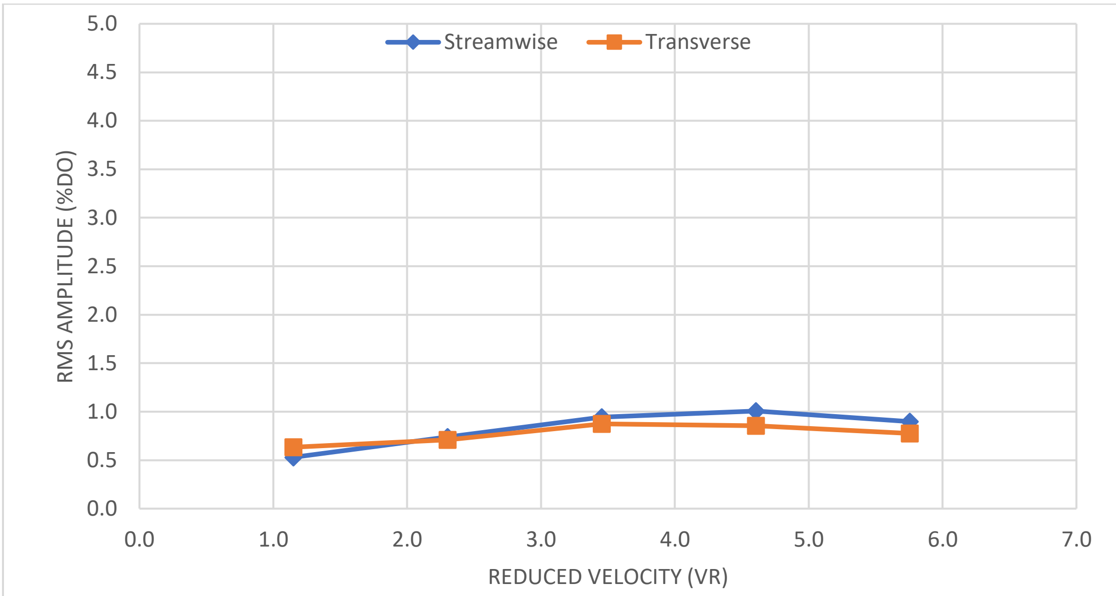

GRAPH 10.7: LIFT AND DRAG AMPLITUDE

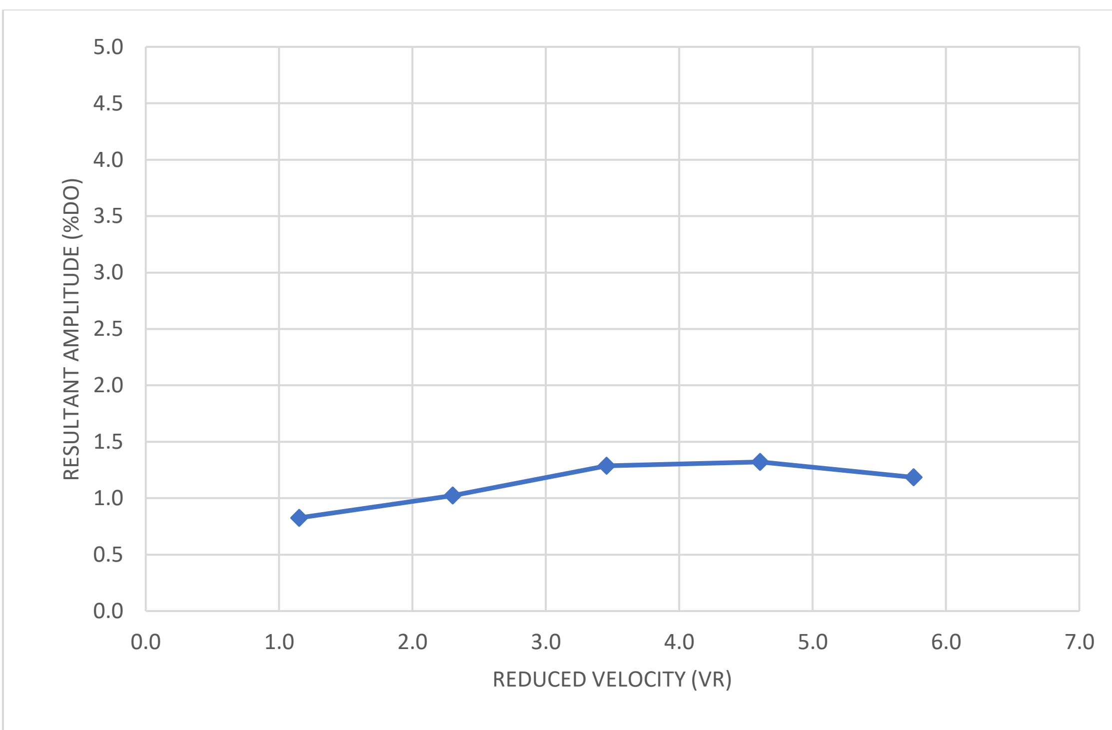

GRAPH 10.8: RESULTANT AMPLITUDE

Chapter 11 Conclusion:

The Water Tunnel has been Fabricated as designed by the designed parameters and requirements.

- The Water Tunnel's designed maximum velocity is 0.7m/s after losses.
- The water tunnel was designed for a maximum test-section velocity of 0.7 m/s; experimentally, a maximum velocity of 0.5 m/s was achieved
- Total Head Loss obtained is 7.8478 m which was suitable for a 5 HP pump but due to its unavailability a 10 HP pump was used.
- The Water Tunnel is well prepared as a (Particle Image Velocimetry) PIV apparatus to be used in potential future Flow Visualization experiments by the fluids lab.
- The flow visualization can be observed by naked eye through dry observation due to low speeds (0.1 – 0.5 m/s).
- It can be used for educational purposes and further experimentation to investigate Flow Fluctuations, Boundary Layer and Vortex Shedding.

For the Validation part of the Water Tunnel,

- The effect of streamwise and transverse amplitude of vibration on a single flexible tube with pitch ratio of 1.54 subjected to water crossflow indicate that the lowest response was noted on the lowest velocity of 0.1m/s.
- And Instability was observed both in streamwise and transverse direction in all four rows, but highest value was recorded in the 3^{rd} row.
- Moreover, in the 3^{rd} row an early instability is propagated, on the flexible tube specifically in transverse amplitude of vibration.

Chapter 12 Bibliography:

[1] S. J. Price, D. Sumner, J. G. Smith, K. Leong, and M. P. Païdoussis, "FLOW VISUALIZATION AROUND A CIRCULAR CYLINDER NEAR TO A PLANE WALL," *Journal of Fluids and Structures*, vol. 16, no. 2, pp. 175–191, Feb. 2002, doi: 10.1006/JFLS.2001.0413.

[2] … E. D.-O.-I. and undefined 2009, "Non-intrusive experimental investigation of flow behavior inside a 5x5 rod bundle with spacer grids using PIV and MIR," *asmedigitalcollection.asme.org*, Accessed: Jun. 05, 2022. [Online]. Available: https://asmedigitalcollection.asme.org/ICONE/proceedings-abstract/ICONE17/351/339824

[3] "Model Studies for the Design of Open- or Closed-Jet Water Tunnel." https://conservancy.umn.edu/handle/11299/108125 (accessed Jun. 09, 2022).

[4] R. J. Etter, J. M. Cutbirth, S. L. Ceccio, D. R. Dowling, and M. Perlin, “High Reynolds number experimentation in the US Navy’s William B Morgan large cavitation channel,” *Measurement Science and Technology*, vol. 16, no. 9, pp. 1701–1709, 2005, doi: 10.1088/0957-0233/16/9/001.

[5] R. J. Etter, J. M. Cutbirth, S. L. Ceccio, D. R. Dowling, and M. Perlin, “High Reynolds number experimentation in the US Navy’s William B Morgan large cavitation channel,” *Measurement Science and Technology*, vol. 16, no. 9, pp. 1701–1709, Sep. 2005, doi: 10.1088/0957-0233/16/9/001.

[6] M. Wosnik and R. Arndt, “Testing of a 1: 6 Scale Physical Model of the Large, Low-Noise Cavitation Tunnel (LOCAT),” no. November, p. 78, 2006, [Online]. Available: https://conservancy.umn.edu/bitstream/handle/11299/113693/pr486.pdf?sequence=1&isAllowed=y

[7] R. E. A. Arndt, V. H. Arakeri, and H. Higuchi, “Some observations of tip-vortex cavitation,” *Journal of Fluid Mechanics*, vol. 229, pp. 269–289, 1991, doi: 10.1017/S0022112091003026.

[8] S. A. Mäkiharju *et al.*, “On the scaling of air entrainment from a ventilated partial cavity,” *Journal of Fluid Mechanics*, vol. 732, no. October, pp. 47–76, 2013, doi: 10.1017/jfm.2013.387.

[9] I. Nedyalkov, “Design of Contraction , Test Section , and Diffuser for a High-Speed Water Tunnel,” pp. 1–80, 2012.

[10] J. B. Leroux, J. A. Astolfi, and J. Y. Billard, “An experimental study of unsteady partial cavitation,” *Journal of Fluids Engineering, Transactions of the ASME*, vol. 126, no. 1, pp. 94–101, 2004, doi: 10.1115/1.1627835.

[11] B. Gindroz and M. L. Billet, “Influence of the nuclei on the cavitation inception for different types of cavitation on ship propellers,” *Journal of Fluids Engineering, Transactions of the ASME*, vol. 120, no. 1, pp. 171–178, 1998, doi: 10.1115/1.2819643.

[12] F. E. Dsm, “Conceptual Design of the Flow Noise Simulator,” pp. 1–5, 2005.

[13] G. F. Oweis, J. Choi, and S. L. Ceccio, “Dynamics and noise emission of laser induced cavitation bubbles in a vortical flow field,” *J Acoust Soc Am*, vol. 115, no. 3, pp. 1049–1058, 2004, doi: 10.1121/1.1646402.

[14] G. C. Lauchle and G. B. Gurney, “Laminar boundary layer transition on a heated underwater body,” *Journal of Fluid Mechanics*, vol. 144, pp. 79–101, 1984, doi: 10.1017/S0022112084001518.

[15] N. K. Madavan, S. Deutsch, and C. L. Merkle, “Reduction of turbulent skin friction by microbubbles,” *The Physics of Fluids*, vol. 27, no. 2, p. 356, Sep. 1998, doi: 10.1063/1.864620.

[16] S. Deutsch and J. Castano, “Microbubble skin friction reduction on an axisymmetric body,” *The Physics of Fluids*, vol. 29, no. 11, p. 3590, Sep. 1998, doi: 10.1063/1.865786.

[17] A. A. Fontaine and S. Deutsch, “The influence of the type of gas on the reduction of skin friction drag by microbubble injection,” *Experiments in Fluids*, vol. 13, no. 2–3, pp. 128–136, 1992, doi: 10.1007/BF00218158.

[18] B. R. Elbing, L. Daniel, Y. Farsiani, and C. E. Petrin, “Design and Validation of a Recirculating, High-Reynolds Number Water Tunnel,” *Journal of Fluids Engineering, Transactions of the ASME*, vol. 140, no. 8, pp. 1–6, 2018, doi: 10.1115/1.4039509.

[19] A. Okajima, T. Kosugi, and A. Nakamura, “Experiments on flow-induced in-line oscillation of a circular cylinder in a water tunnel (1st-report, the difference of the response characteristics when a cylinder is elastically supported at both ends and cantilevered),” *JSME International Journal, Series B: Fluids and Thermal Engineering*, vol. 44, no. 4. pp. 695–704, 2001. doi: 10.1299/jsmeb.44.695.

[20] R. C. Darfler and W. W. Tsai, “Method for a low-cost hydrokinetic test platform: An open-source water flume,” *ASEE Annual Conference and Exposition, Conference Proceedings*, vol. 2017-June 2017, doi: 10.18260/1-2--28665.

[21] M. Saeed, E. Uddin, A. Mubashar, S. Uddin Zahir, C. Islamabad, and P. Ali Abbas Zaidi, “Design and development of low-speed water tunnel,” *ieeexplore.ieee.org*, doi: 10.1109/IBCAST.2018.8312288.

[22] B. R. Elbing, L. Daniel, Y. Farsiani, and C. E. Petrin, “Design and Validation of a Recirculating, High-Reynolds Number Water Tunnel,” *Journal of Fluids Engineering, Transactions of the ASME*, vol. 140, no. 8, pp. 1–6, 2018, doi: 10.1115/1.4039509.

[23] R. Wulandana, “Open water flume for fluid mechanics lab,” *Fluids*, vol. 6, no. 7, 2021, doi: 10.3390/fluids6070242.

[24] Y. el Sayed M., R. Semaan, and R. Radespiel, “Open loop control on a coanda flap water tunnel model,” *35th AIAA Applied Aerodynamics Conference, 2017*, 2017, doi: 10.2514/6.2017-3247.

[25] “Chalmers Open Digital Repository: Design of Contraction, Test Section, and Diffuser for a High-Speed Water Tunnel.” https://odr.chalmers.se/handle/20.500.12380/174857 (accessed Jul. 15, 2022).

[26] H. Kalyankar, R. Melwanki, D. Choudhary, S. Jethwa, and D. Chaudhari, “Design and Analysis of Low-Speed Water Tunnel for Flow Visualization of Bluff Body”.

[27] Q. Yang and Q. Yang, “Experimental investigation of hydraulic characteristics and energy dissipation in a baffle-drop shaft,” *Water Science and Technology*, vol. 82, no. 8, pp. 1603–1613, Oct. 2020, doi: 10.2166/WST.2020.441.

[28] E. Demirel and M. M. Aral, “Liquid Sloshing Damping in an Accelerated Tank Using a Novel Slot-Baffle Design,” *Water 2018, Vol. 10, Page 1565*, vol. 10, no. 11, p. 1565, Nov. 2018, doi: 10.3390/W10111565.

[29] J. Cabonce, H. Wang, and H. Chanson, “Ventilated Corner Baffles to Assist Upstream Passage of Small-Bodied Fish in Box Culverts,” *Journal of Irrigation and Drainage Engineering*, vol. 144, no. 8, p. 04018020, Jun. 2018, doi: 10.1061/(ASCE)IR.1943-4774.0001329.

[30] H. Werle, M. G.-I. its L. Rech. Aerospatiale, and undefined 1976, “Study by hydrodynamic visualisations of various processes for controlling separated flows,” *ui.adsabs.harvard.edu*, Accessed: Jun. 05, 2022. [Online]. Available: https://ui.adsabs.harvard.edu/abs/1976ReAeB.......26W/abstract

[31] J. Rottman, J. S.-J. of F. Mechanics, and undefined 1983, “Gravity currents produced by instantaneous releases of a heavy fluid in a rectangular channel,” *cambridge.org*, pp. 95–110, 1983, Accessed: Jun. 05, 2022. [Online]. Available: https://www.cambridge.org/core/journals/journal-of-fluid-mechanics/article/gravity-currents-produced-by-instantaneous-releases-of-a-heavy-fluid-in-a-rectangular-channel/D2874537091096C7C710F2880077746F

[32] D. I. Pullin and A. E. Perry, “Some flow visualization experiments on the starting vortex,” *Journal of Fluid Mechanics*, vol. 97, no. 2, pp. 239–255, 1980, doi: 10.1017/S0022112080002546.

[33] J. H. Faler and S. Leibovich, “Disrupted states of vortex flow and vortex breakdown,” *Physics of Fluids*, vol. 20, no. 9, pp. 1385–1400, 1977, doi: 10.1063/1.862033.

[34] “Development and Use of a Dynamic-Testing Capability for the DSTO Water Tunnel.” https://apps.dtic.mil/sti/citations/ADA458341 (accessed Jun. 05, 2022).

[35] “An Assessment of the Usefulness of Water Tunnels for Aerodynamic Investigations.” https://apps.dtic.mil/sti/citations/ADA582450 (accessed Jun. 05, 2022).

[36] M. D. Zeiger, O. K. Rediniotis, M. J. Donnelly, and D. P. Telionis, “Temporal evolution of the flowfield over a pitching tangent ogive cylinder,” *33rd Aerospace Sciences Meeting and Exhibit*, 1995, doi: 10.2514/6.1995-441.

[37] H. Huisseune, C. T’Joen, P. de Jaeger, A. Willockx, and M. de Paepe, “Study of junction flows in louvered fin round tube heat exchangers using the dye injection technique,” *Experimental Thermal and Fluid Science*, vol. 34, no. 8, pp. 1253–1264, Nov. 2010, doi: 10.1016/J.EXPTHERMFLUSCI.2010.05.006.

[38] “Water Tunnel Flow Visualisation of Vortex Breakdown Over the F/A-18.” https://apps.dtic.mil/sti/citations/ADA236026 (accessed May 27, 2022).

[39] M. Lang, U. Rist, and S. Wagner, “Investigations on controlled transition development in a laminar separation bubble by means of LDA and PIV,” *Experiments in Fluids*, vol. 36, no. 1, pp. 43–52, Jan. 2004, doi: 10.1007/S00348-003-0625-X/FIGURES/19.

[40] C. Vidali *et al.*, “Wind-tunnel experiments on atmospheric heavy gas dispersion: Metrological aspects,” *Experimental Thermal and Fluid Science*, vol. 130, p. 110495, Jan. 2022, doi: 10.1016/J.EXPTHERMFLUSCI.2021.110495.

[41] S. N. Kasarova, N. G. Sultanova, C. D. Ivanov, and I. D. Nikolov, “Analysis of the dispersion of optical plastic materials,” *Opt Mater (Amst)*, vol. 29, no. 11, pp. 1481–1490, Jul. 2007, doi: 10.1016/J.OPTMAT.2006.07.010.

[42] “Technical Specification for Acrylic sheets.” https://www.cutmyplastic.co.uk/acrylic-technical-specification/ (accessed May 27, 2022).

[43] “Glass Density Evidence - Chemistry LibreTexts.” https://chem.libretexts.org/Ancillary_Materials/Exemplars_and_Case_Studies/Exemplars/Forensics/Glass_Density_Evidence (accessed May 27, 2022).

[44] F. White, *Fluid mechanics*. 1979. Accessed: Jul. 17, 2022. [Online]. Available: https://books.google.com/books?hl=en&lr=&id=zxsGt2OvTo0C&oi=fnd&pg=PR11&dq=frank+m+white+fluid+mechanics+7th+ed+book&ots=DUGhzZh7gt&sig=wpKeCI-6Gu2oq-SbrgDpHkysIW4